BABEŞ-BOLYAI UNIVERSITY
CLUJ-NAPOCA

GHENT UNIVERSITY

Luminescence dating of Romanian loess using feldspars

ŞTEFAN VASILINIUC

PhD Thesis - SUMMARY

Promotors:

Prof. Dr. Constantin Cosma

(Babeş-Bolyai University)

Prof. Dr. Peter van den haute

Dr. Dimitri Vandenberghe

(Ghent University)

Academic year: 2010-2011

The research results discussed in the present thesis have been obtained through the joint PhD collaboration between Babeş-Bolyai University in Cluj Napoca and Ghent University. Ştefan Vasiliniuc performed a total of 14 months of study stay at Ghent University as a PhD student.

The financial support provided by (1) The SECTORAL OPERATIONAL PROGRAMME HUMAN RESOURCES DEVELOPMENT, Contract POSDRU 6/1.5/S/3 – Doctoral studies: through science towards society and (2) Ghent University – Special Research Fund – co-funding for joint doctorate students is highly acknowledged.

Luminescence research of European loess at Ghent University is financed by the Fund for Scientific Research – Flanders (FWO Vlaanderen).

TABLE OF CONTENTS

ABSTRACT

The main objective of this work was to establish an accurate and precise chronology for some of the most important loess sequences in Romania. For this, we investigated the potential of modern and alternative luminescence dating procedures, with the emphasis on feldspar as dosimeter. The first two chapters provide a general introduction into loess deposits and their palaeoclimate significance together with the essential concepts of luminescence as a dating tool. Our first step was to investigate whether the age discrepancy previously observed using different grain-size fractions of quartz is a general characteristic of loess deposits in SE Romania. A detailed investigation of the luminescence characteristics for fine and coarse grained quartz is presented in Chapter III. Further applications of luminescence dating using feldspar as dosimeter are described in the last part of this work. The application of a double-SAR protocol (Chapter IV) showed that this technique is suitable for dating Romanian loess over the last glacial period. Conventional IRSL signals were thoroughly documented in Chapter V. The age results obtained using these signals appear to be affected by contributions from thermally unstable components and/or initial sensitivity changes. The last procedure applied is based on the recently proposed post-IR IRSL protocol (Chapter VI). A Post-IR IRSL signal was identified, that appears to have the capability to extend age range over the last four glacial periods. The results obtained allow an evaluation of feldspar as dosimeter for dating Romanian loess and, at the same time, provide important chronological insights of loess as record of climate change.

Keywords:

- loess
- optically stimulated luminescence (OSL)
- infrared stimulated luminescence (IRSL)
- thermoluminescence (TL)
- quartz
- feldspar
- luminescence dating
- absolute ages
- chronostratigraphy
- palaeoclimate

List of publications

The following ISI papers have been published during the PhD project (October 1st 2008 – September 30th 2011)

1. Timar-Gabor A., **Vasiliniuc Ş.**, Vandenberghe D.A.G. and Cosma C.
   Luminescence dating of archaeological materials and sediments in Romania using quartz.
   Romanian Reports in Physics (2011) 63 (4), in press.
   (impact factor: 0.494)

2. Basarin B., Vandenberghe D.A.G., Marković S.B., Catto N., Hambach U., **Vasiliniuc Ş.**, Derese C., Roncevic S., Vasiljević Dj A., Lj Rajić.
   The Belotinac section (Southern Serbia) at the southern limit of the European loess belt: initial results.
   Quaternary International (2011) 240, 128-138.
   (impact factor: 1.768)

3. Timar-Gabor A., Ivascu C., **Vasiliniuc Ş.**, Daraban L., Ardelean I., Cosma C., Cozar O.
   Thermoluminescence and optically stimulated luminescence properties of 0.5 P2O5 - x BaO - (0.5-x) Li2O glass systems.
   Applied Radiation and Isotopes (2011) 69 (5), 780-784.
   (impact factor: 1.094)

4. **Vasiliniuc Ş.**, Timar Gabor A., Vandenberghe D.A.G., Panaiotu C., Begy R.C., Cosma C.
   A high resolution optical dating study of the Mostiștea loess-palaeosol sequence (SE Romania) using sand-sized quartz.
   Geochronometria (2011) 38(1), 34-41
   (impact factor: 0.860)

5. Timar Gabor A., Vandenberghe D.A.G., **Vasiliniuc Ş.**, Panaiotu C.E., Panaiotu C.G., Dimofte D., Cosma C.
   Optical dating of Romanian loess: a comparison between silt-sized and sand-sized quartz.
   Quaternary International (2011) 240, 62-70.
   (impact factor: 1.768)

6. Timar Gabor A., **Vasiliniuc Ş.**, Badarau A.S., Begy R., Cosma C.
   Testing the potential of optically stimulated luminescence dating methods for dating soil covers from the forest steppe zone in the Transylvanian Basin.
   Carpathian Journal of Earth and Environmental Science (2010) 5, 137 – 144.
   (impact factor: 1.579)

1. Introduction

The major importance of loess deposits as records of climate change has led to an increased number of research studies worldwide. Especially in the past two decades, considerable efforts have been made in refining methods for establishing the chronological framework of loess deposition. Among the several methods applied in the study of loess, luminescence dating provides absolute depositional ages directly, measuring the mineral constituents of the sediment itself. The aeolian nature of loess makes it the perfect material luminescence for the development and testing of luminescence dating methods.

Some of the thickest loess deposits in Europe occur in South-Eastern Romania. These are believed to form the link between the glacial loess deposits of West and Central Europe and the non-glacial loess deposits that extend all the way to China. However, an absolute chronology is generally lacking, the main methods in Romanian loess studies being proxy-based methods (such as pedostratigraphy and magnetic susceptibility).

The establishment of a luminescence research group at Babeş-Bolyai University five years ago took advantage of the latest developments in luminescence dating, namely optically stimulated luminescence (OSL) from quartz corroborated with the single-aliquot regenerative-dose (SAR) protocol. This was successfully applied by Timar et al. (2010) using silt-sized quartz extracted from the loess sequence at Mircea Vodă (Dobrogea). Their results allocated the formation of the uppermost well-developed palaeosol (S1) to the last interglacial period, in agreement with previous studies of similar loess deposits in Romania, Serbia and Bulgaria. Another important outcome of the study of Timar et al. (2010) is the change in loess accumulation rate observed to have happened during the last glacial period. This change in sedimentation rate was correlated with a Marine Isotope Stage (MIS) 3 interstadial during which a weakly developed palaeosol was formed.

A further study of material collected from the sequence at Mircea Vodă was performed using sand-sized quartz grains (Timar et al., 2011). The OSL ages obtained in this study were intriguingly different from those obtained previously using silt-sized quartz. Although both sets of ages allocate the uppermost well-developed palaeosol (S1) to the MIS 5 interglacial, the attribution of the chronological position of the weakly-developed palaeosol observed in the loess unit L1 to either MIS 3 or MIS 5 is disputed. Furthermore, comparison with independent age

control (pedostratigraphy and palaeomagnetism) also indicates that the dating procedure underestimates the true burial age from the penultimate glacial period onwards. Both the age underestimation and the age-discrepancy are not yet understood.

Due to the lack of an independent and absolute age control for Romanian loess, it cannot be evaluated whether any of the quartz-based ages is accurate. This corroborated the need for examining the luminescence characteristics and age of an alternative dosimeter, such as feldspar. Feldspars have the attractive properties of emitting bright luminescence signals that continue to grow up to larger doses. At least in principle, this would allow dating over a larger age range. The advantages, however, may be offset by anomalous fading, a phenomenon that generally affects luminescence signals from feldspars and leads to age underestimation. However, recent studies using modern and alternative procedures have shown that this drawback may be overcome.

Within the framework of this thesis, two directions have been followed. The first direction was to investigate whether the quartz-based OSL ages obtained at Mircea Vodă, reflect a general characteristic of loess deposits in SE Romania. For this, we extended the OSL investigation to the loess sequence near Mostiştea Lake (Danube Plain; SE Romania), by documenting the luminescence characteristics of silt (4-11 µm) and sand-sized (63-90 µm) quartz using the SAR-OSL technique. The second and major research direction adopted in this work was to investigate infra-red stimulated luminescence (IRSL) signals obtained from feldspars extracted from Romanian loess. The investigations included an in-depth study of the luminescence signals from feldspars together with investigations on whether or not it is possible to minimize anomalous fading using newly-reported experimental conditions (e.g. a higher stimulation temperature). Various methodologies for IRSL signals were used, from 'conventional' IRSL and the 'double-SAR' to the most recently developed post-IR IRSL method.

Objectives

The main objective of this work is to establish an accurate and precise chronology for some of the most important loess sequences in Romania. For this, we investigate the potential of modern and alternative luminescence dating procedures, with the emphasis on feldspar as

dosimeter. This is aimed at providing insights into the age discrepancy that the quartz-based OSL studies have shown and also to extend the chronology of these deposits further back in time, beyond the last interglacial/glacial cycle.

Thesis outline

The thesis is composed of six chapters.

Chapter 1 presents a general description of loess and loess deposits and their potential in providing climate change information. A definition of loess and the generally accepted processes that lead to the formation of loess accumulations is given and the variety of information that may be obtained from loess research is briefly reviewed. A geographical perspective is also provided, discussing loess distribution worldwide and in Romania in particular including the study area covered by this work. The previous studies using proxy-based methods are discussed together the chronological interpretation proposed. In addition, this chapter presents the potential of luminescence dating as an absolute method for dating loess deposits together with the previous studies using this method for Romanian loess.

Chapter 2 presents an overview of luminescence dating in short descriptions of the essential concepts: luminescence phenomenon, age equation, dose rate and equivalent dose determination. A general description of feldspars is also included covering mineralogy, advantages for luminescence dating and stimulation and emission spectra. In addition, the IRSL model proposed by Hutt et al. (1988) is presented together with the more recent contributions of Poolton (2002a,b) and Jain and Ankjaergaard (2011). This chapter also includes an overview of anomalous fading covering aspects such as: currently accepted mechanism, detection and correction. In addition, the chapter contains a description of IRSL signals used for dating with respect to thermal stability and measurement procedures applied in dating applications.

Chapter 3 provides an extensive analysis of the luminescence characteristics obtained from both silt-size (4-11µm) and sand-sized (63-80 µm) quartz from the loess section at Mostiștea. The first part presents the general behavior of the two fractions using a single-aliquot regenerative-

dose (SAR) protocol. Equivalent dose and age results are discussed in comparison with the ones previously obtained for the section at Mircea Vodă. The second part of the chapter contains additional investigatins on the reliability of SAR-OSL equivalent doses obtained for quartz samples displaying dose response curves with more than one component.

The following chapters apply different stimulation techniques aimed at investigating signals from feldspar. Polymineral fine grains extracted from samples collected at Mircea Vodă are used as study material.

Chapter 4 presents the application of the double-SAR protocol. The two types of signal obtained using this procedure (IRSL and post-IR OSL) are documented using typical laboratory tests and fading measurements. Age results are compared with the previously ages obtained using silt-sized quartz. A discussion of the advantages and limitations of this procedure is provided.

Chapter 5 presents the investigation of IRSL signals in a conventional approach, involving a stimulation temperature of 50 ^{o}C. The signals are documented using a SAR protocol in terms of thermal stability, initial sensitivity changes and fading. The obtained results are discussed in comparison with previous studies.

Chapter 6 presents the application of the recently reported post-IR IRSL procedure, aimed at obtaining IRSL signals from feldspars that are not affected by anomalous fading. Two types of signal are documented in terms of dose response curve, ability to recover a known given dose and fading. The potential of this procedure is further discussed by comparing age results with the available quartz-based ages and independent age control.

2. Study area

Three of the most representative loess-palaeosol sequences in SE Romania (Fig. 1) were selected for luminescence investigations: near Mostiştea and Costineşti, and Mircea Vodă.

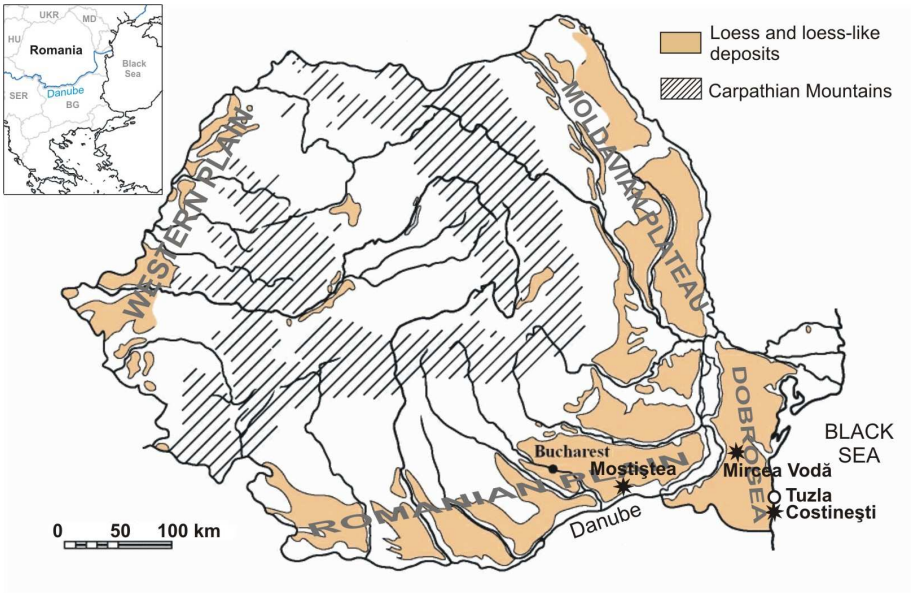

Figure 1: *Distribution of loess and loess-like deposits in Romania showing the location of the study sites and the location of the Tuzla loess section.*

Costineşti

The sequence is located on the coast of the Black Sea (Fig. 1) shore, north of Costineşti village. It comprises at least five loess units (L1-L5) and intercalated palaeosols (S1-S5) plus the Holocene topsoil (S0). A high resolution sampling (10 - 20 cm vertical intervals) was performed for the first two loess layers and S1 unit. The samples collected from the sequence near Costineşti were prepared for the separation of sand-sized (63-90 µm) quartz grains using conventional techniques.

Mostiştea

The loess-palaeosol sequence near Mostiştea is located on the border of Mostiştea lake (~20 km in length and 56.7 km^2 of water surface, Danube Plain, SE Romania; Fig. 1). It is about 21 m thick and consists of four loess-palaeosol units (L1, S1 etc.) and the Holocene topsoil (S0). The two upper palaeosols (S1,S2) are chernozemic while S3 and S4 are brown-reddish palaeosols (Panaiotu et al., 2004).

Mircea Vodă

The sequence at Mircea Vodă is located near the village of Mircea Vodă, in the Dobrogea-plateau (SE Romania) at about 15 km from the River Danube (Fig. 1). It is one of the most complete palaeoclimate archives in Romania. This sequence was the subject of previous luminescence investigations performed by Timar et al. (2010; 2011). It encompasses six loess units (L1-L6), five well-developed palaeosol units (S1-S5) and the Holocene topsoil (S0). In addition, a weakly-developed palaeosol was observed in the L1 loess unit (Timar et al., 2010).

3. Luminescence characteristics of silt-sized and sand-sized quartz: a comparison on the Mostiştea loess-palaeosol sequence (SE Romania)

The Romanian loess-palaesol sequences are thought to represent continuous and extended archives of regional climatic and environmental change during the Late and Middle Pleistocene and they help to improve our understanding of the link between similar deposits in Europe and Asia (Buggle et al., 2009). So far, the chronology of Romanian loess has been mainly based on relative methods (such as pedostratigraphy and magnetic susceptibility) and correlation of successions with comparable features (see e.g. Conea, 1969 and 1970; Panaiotu et al., 2001). It has been demonstrated that the assumptions underlying proxy-based age models (such as continuous sedimentation) can be inaccurate (see e.g. Stevens et al., 2007). Because an absolute timeframe is lacking, there is great uncertainty about the stratigraphic position of several

palaeosols and the way in which they should be correlated. This strongly hampers interpreting the sequences in terms of the signatures of palaeoclimatic and -environmental changes.

As far as Romanian loess is concerned, however, luminescence dating seems to have seen only little application. Balescu et al. (2003; 2010) used infrared stimulated luminescence (IRSL) signals from coarse silt-sized alkali feldspars to establish a broad chronological framework for the loess-palaeosol units exposed at three sections (Tuzla, Mircea Vodă, and near Mostiştea lake; Fig. 1). Despite the limited dataset, these studies demonstrated that, at the three investigated localities, the uppermost well-developed palaeosol (S1) formed during MIS 5.

The most robust luminescence dating procedure currently available involves the use of optically stimulated luminescence (OSL) signals from quartz, in combination with the single-aliquot regenerative-dose (SAR) protocol (Murray and Olley, 2002; Wintle and Murray, 2006). This procedure was applied in the first optical dating applications on Romanian loess, performed by Timar et al. (2010) and Timar Gabor et al. (2011) on the loess-palaeosol sequence at Mircea Vodă (Dobrogea, see Section 2). Their results show a dependency of the age results on the two grain-size fractions of quartz, despite both fractions passing all SAR-procedural tests (i.e. recycling ratio, recuperation and dose recovery; see Timar et al., 2010; Timar Gabor et al., 2011).

In this work we extend the luminescence dating investigations of different grain-size fractions of quartz to the loess-palaeosol sequence at Mostiştea (SE Romania; Section I.6.2). Our main objective is to determine whether there are any discrepancies similar with the results reported by Timar Gabor et al. (2011).

All luminescence measurements were made with a Risø TL/OSL DA-20 reader equipped with blue diodes emitting at 470 ± 30 nm and IR LEDs emitting at 870 nm; luminescence signals were observed through a 7.5 mm thick Hoya U-340 UV filter. Details on the measurement apparatus can be found in Bøtter-Jensen et al. (2003) and Thomsen et al. (2008). Irradiations have been carried out using a ^{90}Sr-^{90}Y beta source. The source was calibrated using calibration quartz supplied by Risø National Laboratory. The dose rate determined for coarse grains deposited on stainless steel disks was 0.161 Gy/s, respectively 0.127Gy/s for fine grains deposited on aluminium disks (reference date August 2011).

The luminescence characteristics of the samples were investigated using the single-aliquot regenerative-dose (SAR) protocol (Murray and Wintle, 2000). Stimulation with the blue

diodes was for 40 s at 125°C. The first 0.32 s of the decay was used in the calculations, minus a background evaluated from the 1.60 s to 2.88 s interval.

Unless indicated otherwise, natural and regenerated signals were measured after a preheat of 10 s at 220°C; the response to the test dose (17 Gy) was measured after a cutheat to 180°C. Timar et al. (2010) and Timar Gabor et al. (2011) used the same thermal pretreatments in their optical dating studies of the loess section near Mircea Vodă. After the measurement of the response to the test dose, a high-temperature bleach was performed by stimulating with the blue diodes for 40 s at 280°C (Murray and Wintle, 2003).

For all samples, the OSL signals obtained from both quartz grain-size fractions are bright and decay rapidly with stimulation time (Fig. 2). The decay is typical for quartz that is dominated by a fast component. This was confirmed by examining the LM-OSL signals of samples from different depths.

To asses the suitability of the employed SAR protocol for measuring the dose in our samples, we performed a dose recovery test. For both quartz fractions the recovered to given dose ratio is generally within 10% from unity (Fig. 3).

Preheat plateau tests have been carried out for for various samples of different age using both grain sizes. No clear dependence of the equivalent dose (D_e) on preheat temperature may be observed across the investigated temperature range (Figs. 4a and b). This is also observed for the corresponding recycling ratios and recuperation (Fig. 4c and d).

The values obtained in the three tests (recycling ratio, recuperation and dose recovery) are usually considered as acceptable in the literature. Therefore, equivalent dose measurements were subsequently performed. Table 1 summarizes the average De values (± 1 standard error) that were obtained using the same SAR protocol as we previously used to date the section near Mircea Vodă (Timar et al., 2010; Timar Gabor et al., 2011).

Radionuclide activity concentrations were obtained through high-resolution gamma-ray spectrometry and converted to dose rates using the conversion factors calculated from the data presented by Adamiec and Aitken (1998).

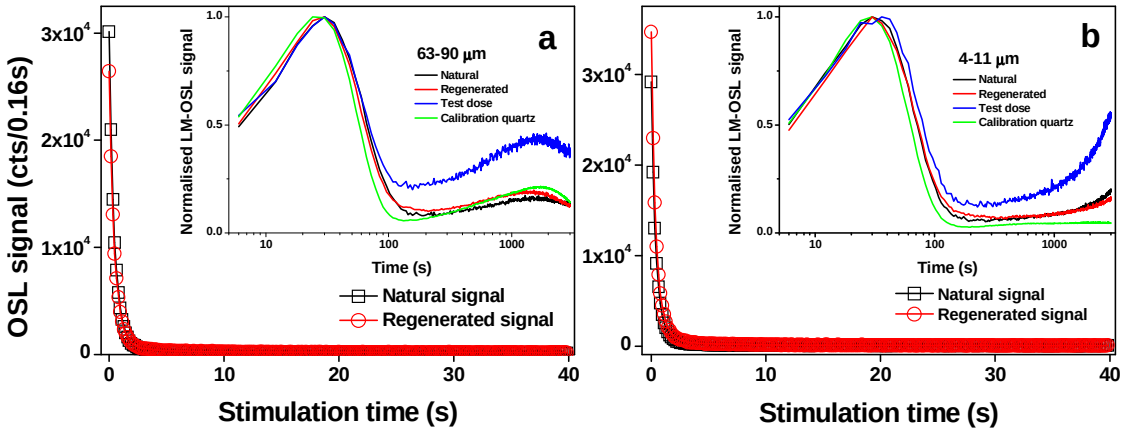

Figure 2: *Examples of natural and regenerated OSL decay curves using sand-sized quartz (a) and silt-sized quartz (b). The signals are measured using aliquots of sample MST2. The insets show natural and regenerated LM-OSL signals obtained using sample MST1 in comparison with calibration quartz. Stimulation power was ramped from 0 to 100% in 3000s. The natural, regenerated and calibration quartz luminescence signals were measured at 125°C, following a preheat of 10 s at 220°C. The test dose signal was measured at 125°C, following a cutheat at 180°C.*

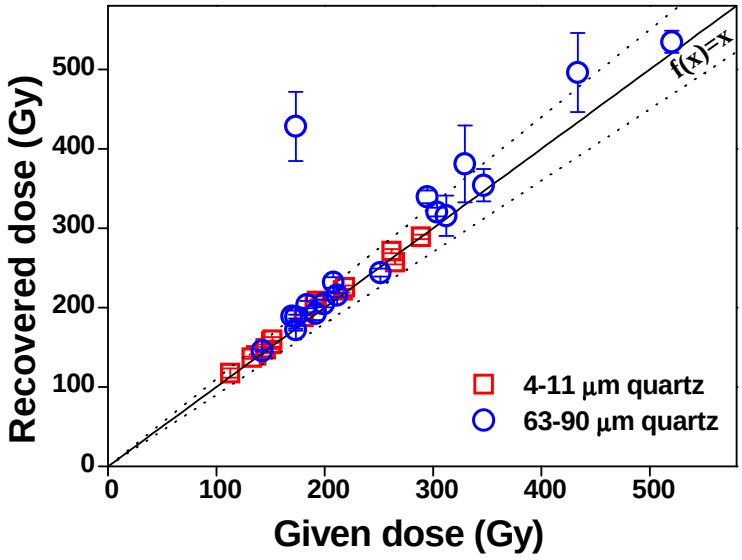

Figure 3: *Results of the dose recovery test obtained using both fine and coarse quartz for the samples collected from Mostiştea. Error bars represent one standard error. The solid and dashed lines are the 1:1 relation and brackets of 10% deviation from unity, respectively.*

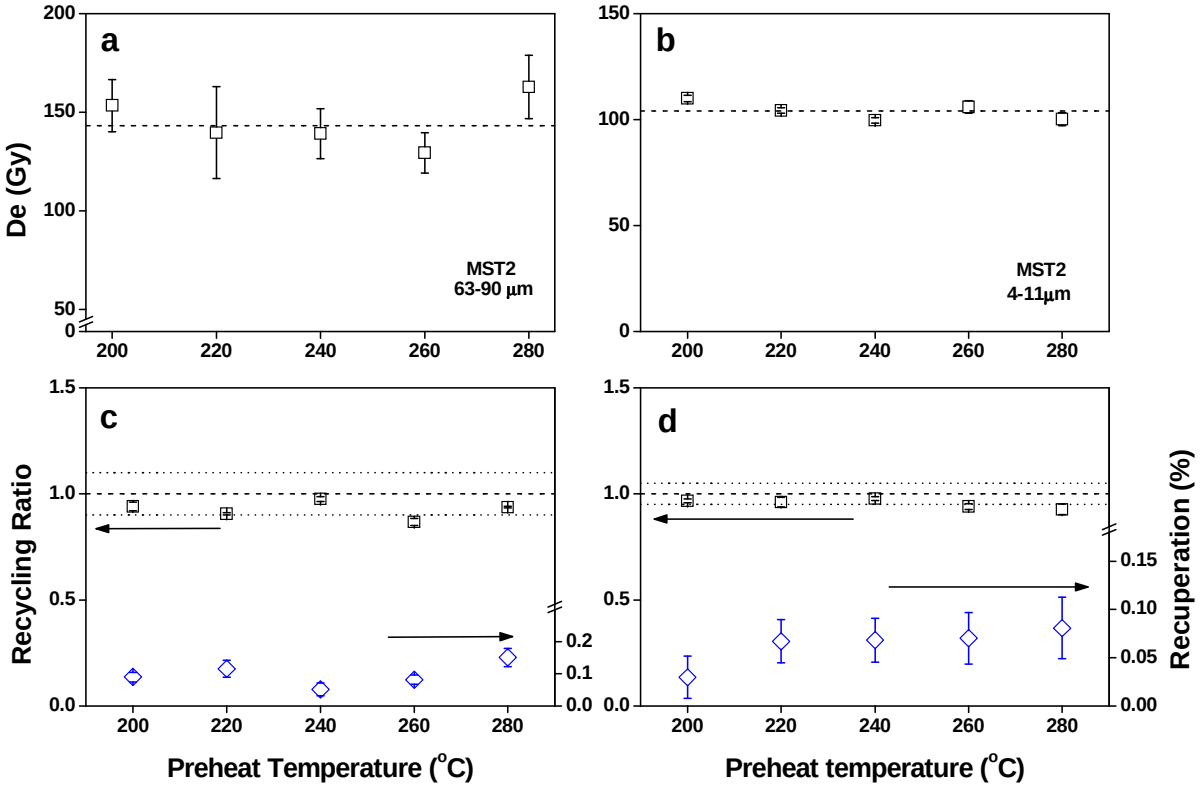

Figure 4: *Equivalent dose as a function of preheat temperature for sample MST2, sand-sized grains (a); silt-sized grains (b). A minimum of three aliquots was used per preheat temperature and the error bars represent one standard error. The dashed line (eye guide) highlights the average value across the 200-280°C preheat temperature interval. (c) and (d) present recycling ratios and recuperation as a function of preheat temperature for the same aliquots as in (a) and (b). Error bars represent one standard errors. The dashed and dotted lines (eye guide) highlight the ideal recycling ratio of unity and a ±10% (c) and ±5% (d), respectively.*

For 63-90 µm grains the external beta dose rates were corrected for the effects of etching and attenuation using a factor of 0.94 (± 5 % relative uncertainty (Mejdahl, 1979). Moreover, an internal dose rate of 0.013 ± 0.003 Gy/ka was assumed (Vandenberghe et al., 2008). In the case of 4-11 µm grains, an a-value of 0.04 ± 0.02 was adopted to allow for the lower efficiency of alpha radiation in inducing luminescence. A water content of 20 ± 5% was used to account for the effect of moisture (Balescu et al., 2003) and the contribution from cosmic radiation was calculated following Prescott and Hutton (1994). Table 1 summarizes the dosimetric information. It can be seen that there is little variation in dose rate with depth and the values are spread around a mean value (± 1 standard error) of 2.84 ± 0.02 Gy/ka and 3.26 ± 0.02 Gy/ka for coarse and fine grains respectively.

Sample	Depth (cm)	Grain size (µm)	^{226}Ra (Bq kg^{-1})	^{232}Th (Bq kg^{-1})	^{40}K (Bq kg^{-1})	Total Dose Rate (Gy / ka)	De (Gy)	Age (ka)	σ_r (%)	σ_{sys} (%)	FG/ CG
MST 1	**210**	**63-90** **4-11**	33 ± 1	40 ± 1	594 ± 8	2.85 ± 0.03 3.31 ± 0.03	**175 ± 8** (n=17/18) **138 ± 2** (n=7/7)	**61 ± 8** **42 ± 6**	5 2	13 14	0.69
MST 2	**220**	**63-90** **4-11**	32 ± 1	41 ± 1	591 ± 8	2.84 ± 0.03 3.29 ± 0.03	**130 ± 10** (n=7/10) **113 ± 2** (n=8/8)	**46 ± 7** **34 ± 5**	7 2	13 14	0.74
MST 3	**232**	**63-90** **4-11**	35 ± 1	41 ± 1	606 ± 8	2.93 ± 0.03 3.40 ± 0.03	**153 ± 4** (n=9/11) **151 ± 4** (n=7/7)	**52 ± 7** **44 ± 6**	3 3	13 14	0.85
MST 4	**242**	**63-90** **4-11**	32 ± 1	40 ± 1	625 ± 6	2.91 ± 0.02 3.36 ± 0.02	**162 ± 18** (n=8/8) **134 ± 2** (n=8/8)	**56 ± 9** **40 ± 6**	11 1	13 14	0.71
MST 5	**256**	**63-90** **4-11**	33 ± 1	41 ± 1	609 ± 8	2.90 ± 0.03 3.36 ± 0.03	**169 ± 9** (n=6/8) **146 ± 1** (n=8/8)	**58 ± 8** **44 ± 6**	5 1	13 14	0.76
MST 6	**267**	**63-90** **4-11**	32 ± 1	39 ± 1	612 ± 9	2.86 ± 0.03 3.30 ± 0.04	**185 ± 9** (n=15/15) **147 ± 2** (n=7/7)	**65 ± 9** **44 ± 6**	5 2	13 14	0.68
MST 7	**278**	**63-90** **4-11**	32 ± 1	41 ± 1	603 ± 8	2.86 ± 0.03 3.32 ± 0.03	**191 ± 17** (n=7/8) **149 ± 3** (n=6/6)	**67 ± 11** **45 ± 6**	9 2	13 14	0.67
MST 8	**293**	**63-90** **4-11**	34 ± 1	41 ± 1	605 ± 8	2.90 ± 0.03 3.36 ± 0.03	**186 ± 12** (n=10/13) **152 ± 2** (n=8/8)	**64 ± 9** **45 ±6**	6 2	13 14	0.70
MST 9	**330**	**63-90** **4-11**	31 ± 1	37 ± 1	593 ± 8	2.76 ± 0.03 3.18 ± 0.03	**260 ± 28** (n=5/17) **X**	**94 ± 16** **X**	11 X	13 X	x
MST 10	**350**	**63-90** **4-11**	31 ± 1	38 ± 1	576 ± 6	2.72 ± 0.02 3.15 ± 0.03	**210 ± 16** (n=5/5) **X**	**77 ± 11** **X**	7 X	13 X	x
MST 11	**375**	**63-90** **4-11**	32 ± 1	37 ± 1	591 ± 8	2.76 ± 0.03 3.19 ± 0.03	**232 ± 33** (n=7/11) **178 ± 4** (n=7/7)	**84 ± 16** **56 ± 8**	14 3	13 14	0.66
MST 12	**400**	**63-90** **4-11**	32 ± 1	39 ± 1	606 ± 8	2.83 ± 0.03 3.27 ± 0.03	**237 ± 22** (n=11/13) **193 ± 2** (n=8/8)	**84 ± 13** **59 ± 8**	9 2	13 14	0.70
MST 13	**425**	**63-90** **4-11**	33 ± 1	41 ± 1	601 ± 8	2.86 ± 0.03 3.31 ± 0.03	**277 ± 15** (n=11/13) **X**	**97 ± 14** **X**	6 X	13 X	x
MST 14	**450**	**63-90** **4-11**	32 ± 1	40 ± 1	621 ± 8	2.88 ± 0.03 3.32 ± 0.03	**273 ± 25** (n=8/8) **191 ± 2** (n=8/8)	**95 ± 15** **58 ± 8**	9 1	13 14	0.61
MST 15	**475**	**63-90** **4-11**	32 ± 1	40 ± 1	618 ± 9	2.86 ± 0.03 3.31 ± 0.04	**253 ± 38** (n=3/6) **217 ± 1** (n=8/8)	**88 ± 18** **66 ± 9**	15 1	13 14	0.75
MST 16	**500**	**63-90** **4-11**	31 ± 1	40 ± 1	589 ± 8	2.77 ± 0.03 3.23 ± 0.03	**275 ± 51** (n=6/10) **219 ± 5** (n=6/6)	**100 ± 22** **68 ± 10**	19 2	13 14	0.68
MST 17	**550**	**63-90** **4-11**	29 ± 1	38 ± 1	557 ± 7	2.63 ± 0.02 3.03 ± 0.03	**279 ± 28** (n=5/6) **265 ± 5** (n=7/7)	**107 ± 18** **87 ± 12**	10 2	13 14	0.81
MST 18	**575**	**63-90** **4-11**	30 ± 1	38 ± 1	585 ± 6	2.70 ± 0.02 3.11 ± 0.03	**391 ± 28** (n=5/6) **252 ± 3** (n=11/11)	**144 ± 21** **81 ± 12**	7 2	13 14	0.56
MST 19	**600**	**63-90** **4-11**	29 ± 1	38 ± 1	585 ± 7	2.69 ± 0.02 3.10 ± 0.03	**288 ± 57** (n=4/4) **289 ± 9** (n=6/6)	**107 ± 26** **93 ± 14**	20 3	13 14	0.87

Table 1: *Summary of radionuclide activities, calculated total dose rates, equivalent doses (D_e), optical ages, and random (σ_r) and systematic (σ_{sys}) uncertainties. The number of accepted aliquots out of the total measured is indicated in the subscript to the D_e-data. Uncertainties mentioned with the D_e and dosimetry data are random; all uncertainties represent one sigma. The uncertainty associated with the water content (20 ± 5 %) is dominant in the overall systematic uncertainty. The ratio of the age results obtained using the fine grains (FG) to the coarse grains (CG) is given in the last column.*

For all investigated samples, the ages obtained using the 4-11 µm quartz appear systematically younger than the ages obtained using the 63-90 µm quartz, with an age difference ranging from ~ 13 to 44 % (see Table III.1).

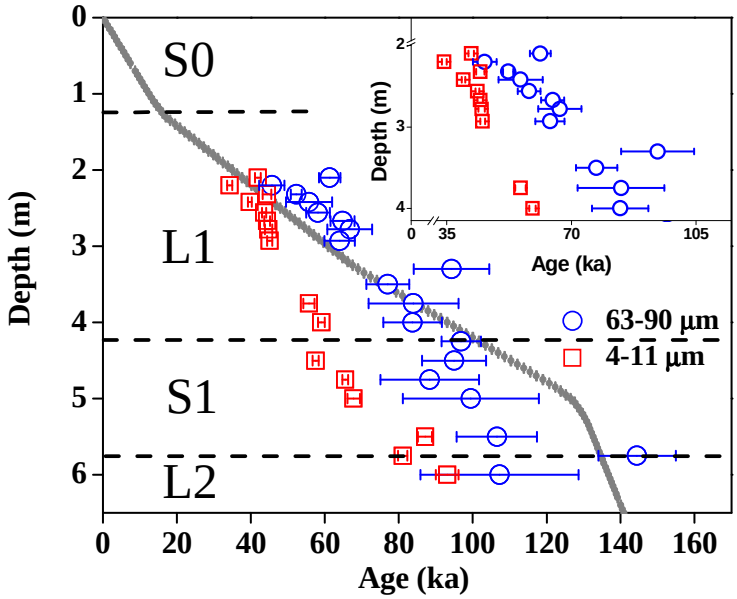

Figure 5: *Plot of optical ages (1 sigma total uncertainties) from silt-sized (open squares) and sand-sized (open circles) quartz grains. The magnetic age-depth model is shown by the dotted line with error bars incorporating a depth error of ± 10 cm for the correlation between the section investigated here and the one for which the model was established (Necula and Panaiotu, 2008). The dashed lines (eye guide) highlight the boundaries of the stratigraphic units. The inset shows the optical ages (1 sigma random uncertainties) obtained for the L1 unit.*

The age discrepancy appears to be related to the difference in D_e values obtained using the two quartz fractions. The D_e values obtained for sand-sized quartz are systematically higher than the values obtained for the silt-sized quartz with no apparent dependence on the stratigraphic position of the samples (Table). Timar Gabor et al. (2011) obtained similar results for the loess sequence Mircea Voda section. These results are very concerning as the equivalent

doses obtained on coarse-grained etched quartz should be smaller than those obtained on the fine grains when considering the effective dose rates.

The previous investigations on fine (4-11μm) and coarse (63-90 μm) grained quartz samples from the loess section near Mircea Vodă (SE Romania), showed a higher than exponential pattern of growth for the dose response (Timar et al., 2010; Timar Gabor et al., 2011). As very different patterns of growth were observed for the two grain sizes for regenerative doses applied up to 700 Gy, the present work aims at deepening these investigations by analising the dose response pattern in the very high dose region 5000-10000Gy. Luminescence charactersitics of fine and coarse quartz extracted from Mostiştea section will be documented along with new data from Mircea Vodă in order to gain more insights into the equivalent dose discrepancy obtained for the two fractions.

Fig. 6 shows extended dose response curves using regenerative doses up to 10 kGy obtained for two samples from the loess sequence at Mircea Vodă.

In both cases, the fits were best with a DSE function as indicated by the reduced chi square values as well as the residual sums of squares (see Table 2). However, it can be noticed as well that the saturation characteristics of the two grain sizes are very different, the coarse grains saturating much earlier.

Regression model	**Data points used**	**Degrees of freedom**	**Reduced χ^2**	**Residual sums of squares**
MV 10 4-11 μm				
SSE	14	11	0.92	10
DSE	14	9	0.085	0.76
MV 8 63-90 μm				
SSE	14	11	0.162	1.8
DSE	14	9	0.05	0.5

Table 2: *Comparison between the goodness of fit using a SSE and a DSE regression model for dose-response curves constructed up to 10000 Gy for samples collected from the loess-sequence at Mircea Vodă.*

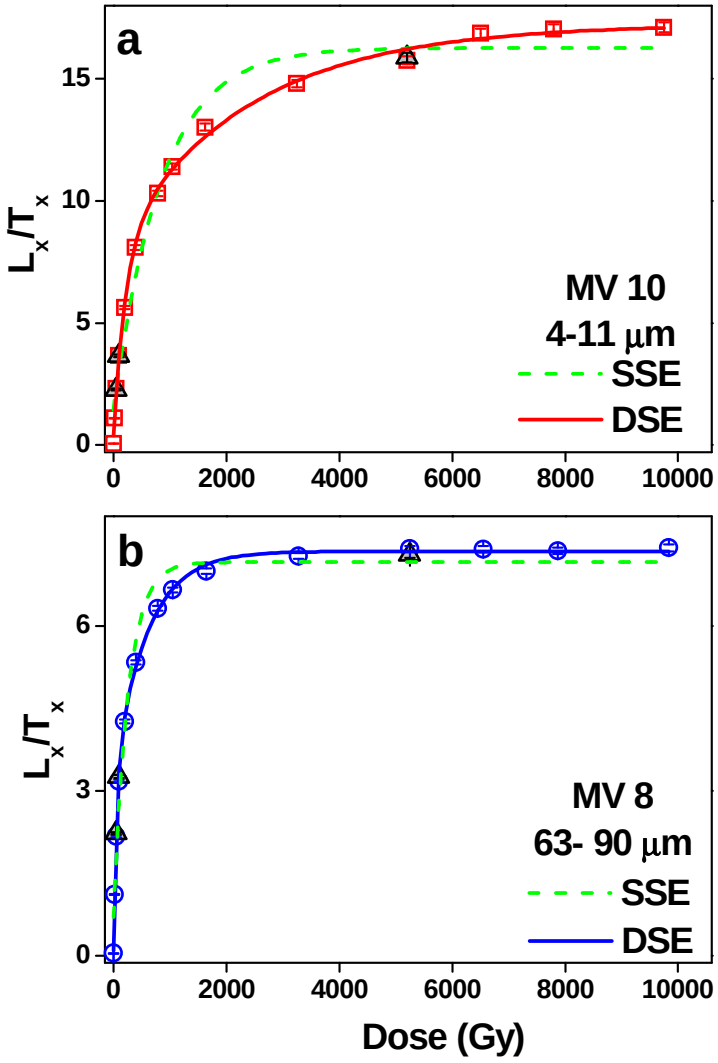

Figure 6: *Comparison between sensitivity corrected growth curves constructed using silt-sized quartz (a) and sand-sized quartz (b) extracted from samples collected from Mircea Vodă. The L_x/T_x data are fitted with either a single saturating exponential (SSE) or a double saturating exponential (DSE) function. Recycled points are shown as grey-filled triangles.*

Dose response curves were obtained up to 5000 Gy for both coarse and fine grains from a number of samples from site MST (Fig. 7). The growth of the signal with dose is best represented by the sum of two saturating exponential functions for all samples investigated. The coarse grain samples (MST 3, 7 and 19) show negligible growth when doses above 1000 Gy are used. This is in contrast to the continuing growth shown by the fine grain samples (MST2, MST6, MST 13, MST 19). There appears to be a fundamental difference in response between fine and coarse grained quartz when doses up to 5000 Gy are used to construct dose response curves.

The saturation characteristics for all the data plotted in Fig. 7 is summarized in Table 3. The values for the characteristic doses D_{01} and D_{02} do not seem to vary with the stratigraphic depth of the sample but are very different for the two different grain size fractions. Timar Gabor et al. (2011) made the same observation for samples collected at Mircea Vodă.

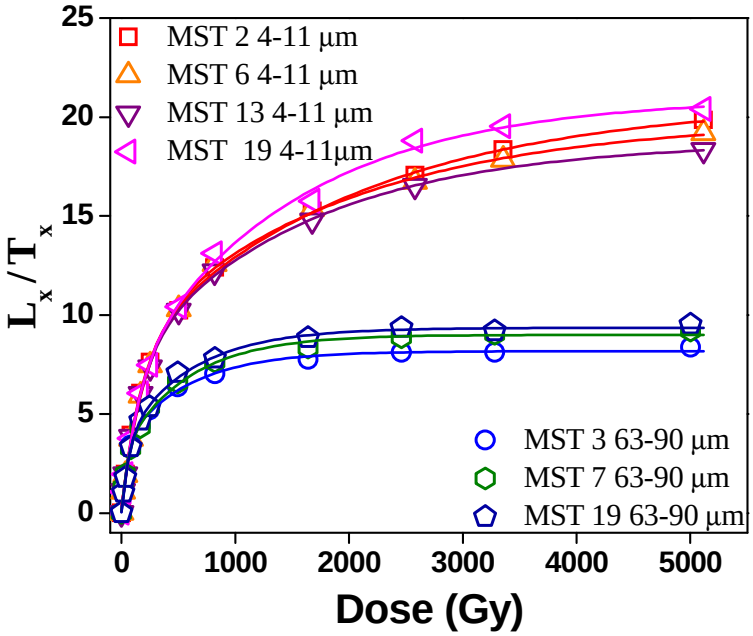

Figure 7: *Dose response curves constructed using silt- and sand-sized quartz extracted from different samples from Mostiştea. The solid lines represent the best fit to the sum of two saturating exponential functions.*

SAMPLE	I_0	A	D_{01}	B	D_{02}	Red. χ^2	RSS
MST 2 4-11 µm	0.2±0.1	7.7 ± 0.5	168 ± 16	12.9 ±0.4	2031 ± 202	0.032	0.22
MST 6 4-11 µm	0.3±0.2	8.3 ± 0.7	200 ± 24	11.3 ± 0.5	1917 ± 280	0.047	0.33
MST 13 4-11 µm	0.2 0.1	7.3 ± 0.6	164 ±18	11.2 ± 0.5	1588 ±163	0.003	0.19
MST 19 4-11 µm	0.2±0.2	6.5 ± 1.0	154 ± 35	14.3 ± 0.8	1500 ± 216	0.109	0.76
MST 3 63-90 µm	0.1±0.1	3.5 ± 0.3	53 ± 9	4.6 ± 0.3	576 ± 69	0.019	0.14
MST 7 63-90 µm	0.1±0.2	3.1 ± 0.4	49 ± 12	5.8 ± 0.4	586 ± 64	0.036	0.25
MST 19 63-90µm	0.1±0.1	3.6 ± 0.4	66 ± 13	5.7 ± 0.4	600 ± 72	0.024	0.17

Table 3: *Fitting parameters for OSL dose response of samples of different ages from Mostistea*

In order to test whether the difference in dose response curves has an effect when an infinitely old sample is measured, we have constructed the dose response for sample CST_{inf}, collected below palaeosol unit S6 at Costinesti section. This sample and is expected to be at least 800 Ka years old and thus one will assume that quartz OSL signals are in saturation. When the

same two grain sizes were extracted and measured, once again, the dose response curve for the coarse grains showed negligible growth above 1000 Gy (Fig. 8a), whilst this was observed for fine quartz only above 4000 Gy (Fig. 8b). Within 1 standard error, the values of De obtained were identical, both being much lower than expected from the geological context of the sample; the natural value of L/T was below the saturation level for both quartz. Furthermore, a dose recovery experiment was carried out on fine grains using a dose of 1,170 Gy and this could be recovered within 1%.

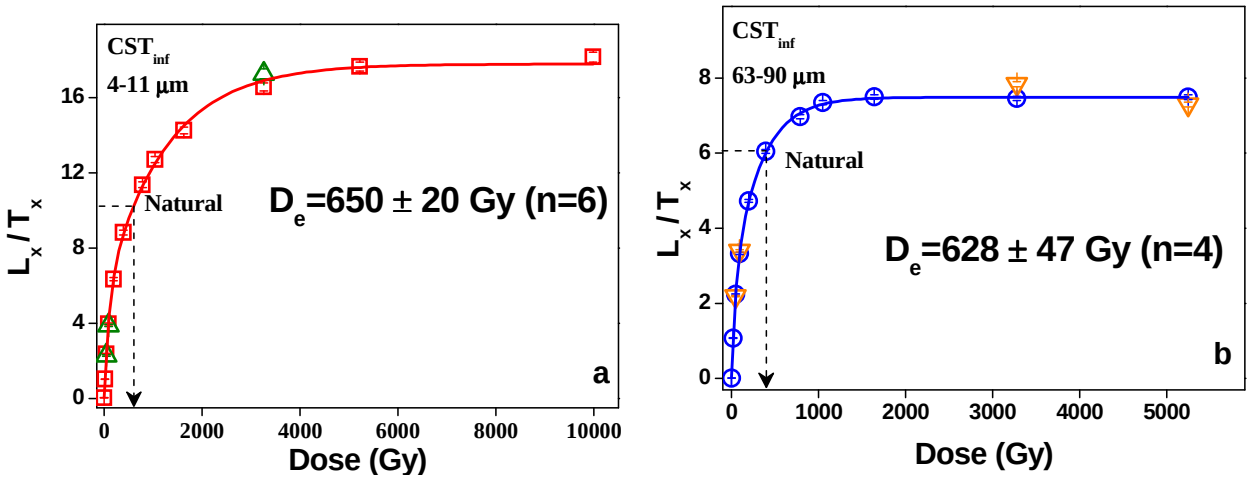

Figure 8: *Extended dose-response curves obtained for sample CST_{inf} using fine (a) and coarse (b) quartz. Recycling points are shown as triangles. The average equivalent dose obtained for each fraction is indicated as well.*

Our study of quartz extracted from the loess sequence at Mostistea used the same methodology as the one used in the studies of Timar et al. (2010) and Timar Gabor et al. (2011) for Mircea Voda section. The signals selected for analysis from both grain-size fractions of quartz appear very similar with the ones investigated for samples at Mircea Voda. The dominance of the fast component in the OSL signals is indicated by the decay shape of the CW-OSL and LM-OSL signals. Furthermore, both quartz fractions passed the procedural tests of the single-aliquot regenerative-dose (SAR) protocol (i.e. recycling ratio, recuperation and dose recovery up to a given dose of 1200 Gy) indicating that the protocol should provide reliable D_e values. High resolution pulse anneal experiments exclude a possible contribution from a thermally unstable component to the OSL signals from both fractions. Additionally, preliminary fading experiments confirm the stability of the investigated signal. However, the age results

obtained for the two fractions are generally inconsistent. The age discrepancy resides in the D_e values obtained for the two quartz fractions.

In the case of the samples investigated from Mostistea section all the equivalent doses determined (at least for the 63-90μm) fraction are obtained by interpolating on a region of the dose response where the first exponential function is already in saturation (D_e (63-90 μm) > $2D_{01}$ =110 Gy). We believe that more work is needed for conceptualising the process, independent processes or set of competing processes that generate the double exponential saturating behaviour of quartz OSL in order for these equivalent doses to be considered reliable.

Our results from the quartz-based OSL study at Mostistea indicate that the age discrepancy observed between two grain sizes of quartz may be characteristic for loess deposits in SE Romania. The source of this discrepancy remains yet unexplained. Our data confirm the fact that the linear tem increasingly reported in literature for quartz OSL dose response up to 1000 Gy is the expression of a second later saturating exponential function. The presence of an additional function, besides a single saturating exponential, in the dose response curves constructed for both types of quartz grains, may indicate that there are still unknown processess that influence the characteristics of the signals used for age determination. Therefore, these results suggested that the reliability of the age results obtained from signals with similar saturation characteristics of the dose response curve should be regarded with caution.

4. Combined IRSL and post-IR OSL dating of Romanian loess using single aliquots of polymineral fine grains

This work focuses on the luminescence characteristics and ages obtained for polymineral fine (4-11 μm) grains extracted from the loess-palaeosol sequence near Mircea Vodă. A 'double-SAR' protocol (Banerjee et al., 2001; Roberts and Wintle, 2001) is used for equivalent dose (D_e) determination. This protocol involves observing an infrared stimulated luminescence (IRSL) signal from the feldspathic component of the mineral mixture, followed by that of an optically stimulated luminescence signal (post-IR OSL) that is thought to originate mainly with the quartz constituent. We investigated this approach because (i) it may allow obtaining reliable age results while avoiding the chemical separation process during sample preparation, and (ii) the feldspar-

IRSL ages may provide an independent age check on the OSL ages previously obtained using silt-sized quartz.

The loess-palaeosol sequence near Mircea Vodă (SE Romania) is one of the most complete palaeoclimate archives in Romania (see Section 1). Twelve samples were taken from the loess units corresponding to the last four glacial periods. Nine samples (GLL-071801 to -09) were collected from the L1 loess unit while one sample was collected from each of the three loess units below (GLL-071810 from L2, -12 from L3 and -13 from L4). A complete description of the study site and sample collection can be found in Timar et al. (2010; 2011).

All luminescence measurements were performed using an automated Risø TL/OSL-DA-12 reader equipped with an infrared (IR; 830 ± 10 nm) laser diode (Bøtter-Jensen and Murray, 1999) and blue (470 ± 30 nm) light emitting diodes (LEDs; Bøtter-Jensen et al., 1999). The UV emission of the luminescence signals was detected through a 7.5 mm thick Hoya U-340 filter.

Table 4 shows the measurement steps and parameters in the protocol as used in this work.

1. Dose	
2. Preheat to 240 °C, for 10 s	
3. IRSL, 100 s at 125 °C	**→ $L_{x,\ IRSL}$**
4. OSL, 100 s at 125 °C	**→ $L_{x,\ post\text{-}IR\ OSL}$**
5. Test dose	
6. Cutheat to 180 °C	
7. IRSL, 100 s at 125 °C	**→ $T_{x,\ IRSL}$**
8. OSL, 100 s at 125 °C	**→ $T_{x,\ post\text{-}IR\ OSL}$**
9. OSL, 40 s at 280 °C	

Table 4: *The double-SAR measurement protocol*.

Fig. 9 shows a representative dose response curve of the IRSL and post-IR OSL signal from an aliquot of sample GLL-071806. In both cases, the natural signal is well below saturation. Fig. 9 also illustrates that sensitivity changes occurring during repeated SAR cycles are accurately corrected for (i.e. recycling ratios are within 0.9-1.1) and that the curves pass close to the origin (implying that recuperation is negligible). The inset in Fig. 9 presents representative decays of IRSL and post-IR OSL signals in comparison with the decay of the OSL signal from

calibration quartz. The post-IR OSL signal appears to decay much slowly than the OSL signal from calibration quartz. Timar et al. (2011) showed that natural OSL signals of pure 4-11 µm quartz extracted from the same samples are indistinguishable from the calibration quartz signals. Therefore, the slower decay of the post-IR OSL signal cannot be derived entirely from quartz. It may however indicate that a significant contribution from the feldspathic component persists in the post-IR OSL signal.

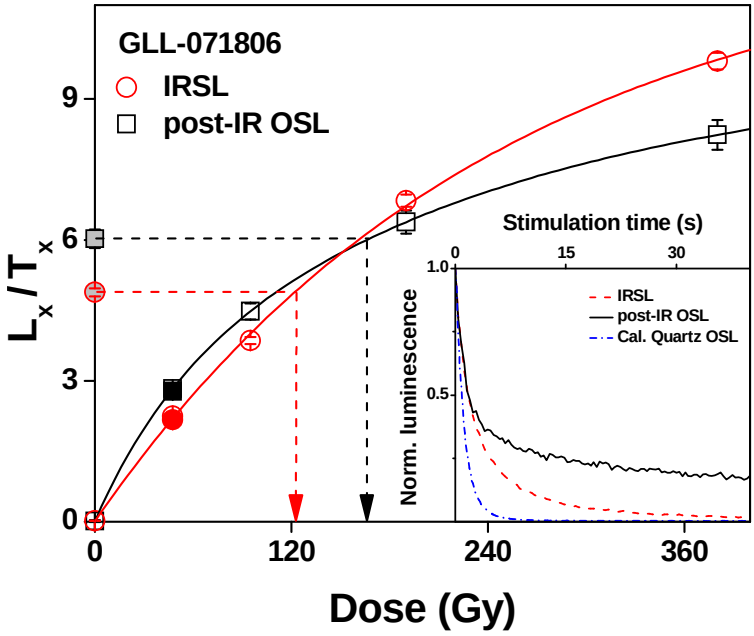

Figure 9: *Dose response curves of the IRSL (open circle) and post-IR OSL signal (open square) from one aliquot of sample GLL-071806. The inset shows representative decay curves of the OSL signal from fine silt-sized (4-11 µm) calibration quartz, and the IRSL and post-IR OSL signals from polymineral fine grains, obtained using sample GLL-071802.*

Laboratory tests (i.e. recycling ratio, recuperation and dose recovery; see Fig.10) indicate that the protocol should be suitable for D_e determination using both IRSL and post-IR OSL signals.

However, fading measurements show that both signals exhibit anomalous fading, indicating indicates that the preceding stimulation with IR diodes does not reduce the contribution from feldspar to a negligible level. This was expected from the shape of the decay curve of this signal in comparison with typical fine silt (4-11 µm) calibration quartz (Fig. 9).

Previous studies have indicated that OSL signals from feldspars may be observed even after IR stimulation (see e.g. Duller and Bøtter-Jensen, 1993; Roberts, 2007; Kim et al., 2009).

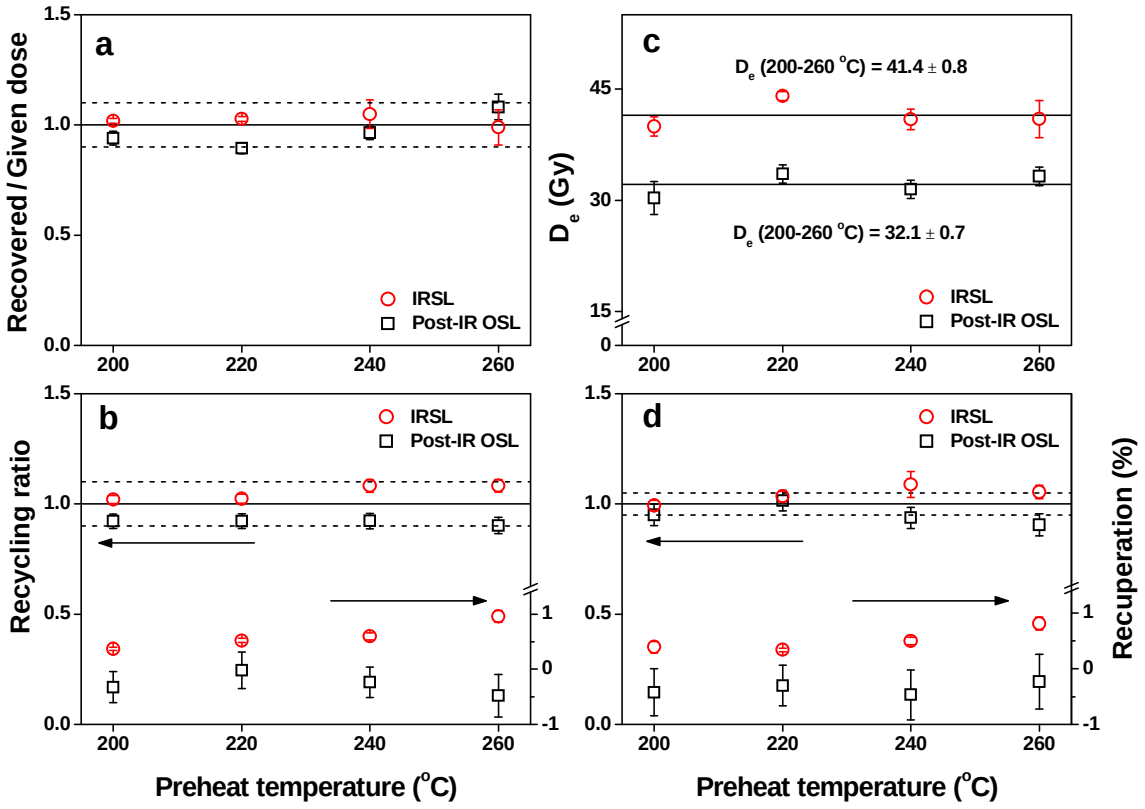

Figure 10: *(a) Variation in recovered/given dose ratio as a function of preheat temperature for sample GLL-071802. (b) Recycling ratios and recuperation corresponding to the data in (a). (c) Variation in equivalent dose (D_e) as a function of preheat temperature for sample GLL-071802 (d) Recycling ratios and recuperation corresponding to the data in (c).*

For the uppermost two samples (GLL-078101 and -02), the fading-corrected IRSL ages are significantly higher than the corrected post-IR OSL ages (Fig. 11); the latter agree well with the quartz-based OSL ages. These two samples were collected from the upper part of the L1 loess unit (Fig. 11), which may have been affected by post-depositional soil formation processes (e.g. bioturbation) during the Holocene. Therefore, the apparent inconsistency may be related to incomplete resetting of the IRSL signal during such reworking; it is well known that feldspar IRSL signals bleach more slowly than quartz (see e.g. Thomsen et al., 2008).

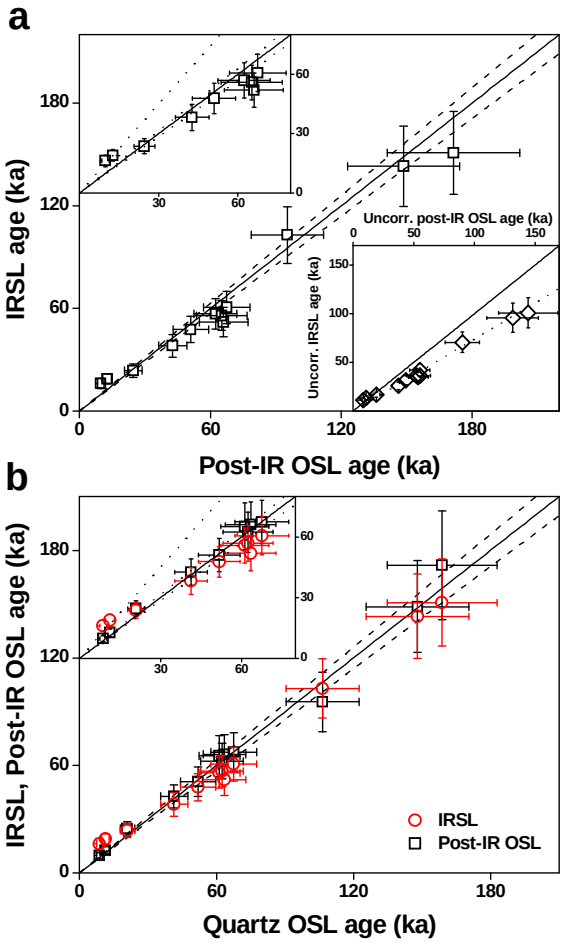

Figure 11: *(a) Comparison between fading-corrected IRSL and fading-corrected post-IR OSL ages. (b) Plot of fading-corrected IRSL and post-IR OSL ages against the quartz OSL ages of Timar et al. (2010).*

For the remainder of the samples, the corrected IRSL ages agree well with the corrected post-IR OSL ages (Fig. 11a) although the two signals appear to be affected by anomalous fading to different extents (Fig. 11a; lower inset). Furthermore, the entire post-IR OSL dataset agrees well with that previously obtained by Timar et al. (2010) using OSL signals from silt-sized quartz. The overall consistency between results obtained for different dosimeters (feldspar and quartz) increases the reliability of age results obtained using fine grains, at least for the samples collected from loess unit L1. As such, they corroborate the correlation of the weakly developed palaeosol in the L1 unit with MIS3.

The quartz OSL ages for the samples collected from the loess units L2, L3 and L4 have previously been interpreted as underestimates of the true burial age (Timar et al., 2010). The

agreement between the OSL and the fading-corrected IRSL ages for these samples is not thought to enhance the reliability of either dataset. Indeed, the fading-correction model is expected to be valid only for samples for which the natural signal falls on the linear region of the dose response curve (Huntley and Lamothe, 2001), a condition which is not met for these samples. As such, both datasets are interpreted as underestimating the true burial age, and their agreement as coincidence.

The excellent agreement between the fading-corrected post-IR OSL ages and the quartz OSL ages (Fig. 11b) suggests that it may not be necessary to chemically separate the fine quartz fraction in order to obtain reliable luminescence ages for Romanian loess. A similar finding was recently reported by Schmidt et al. (2010) using polymineral fine grains extracted from Serbian loess.

We conclude that application of the double-SAR protocol to polymineral fine grains offers a viable alternative for dating Romanian loess, avoiding the need to isolate pure quartz using chemical procedures. The IRSL and post-IR OSL signals exhibit anomalous fading, however, and the ages derived from these signals are therefore dependent on the fading correction model. An agreement between ages obtained using feldspar (IRSL), quartz (OSL) and/or mixed (post-IR OSL) signals increases confidence in the dating results. Our results suggest that use of the double-SAR protocol should be restricted to samples from last glacial period.

5. Conventional IRSL dating of Romanian loess using single aliquots of polymineral fine grains

Using the same study material (polymineral fine grains – 4-11 µm) as in the previous chapter, a conventional IRSL approach is investigated using a single-aliquot regenerative-dose (SAR) protocol (Murray and Wintle, 2000) involving IR stimulation at 50 ^{o}C and detection in the blue region.

All luminescence measurements were performed using a Risø TL/OSL-DA-15 reader. Infrared stimulation used infrared (IR) LEDs emitting at 875 nm and IRSL signals were detected through a BG39/Corning 7-59 filter combination (Bøtter-Jensen et al. 2003). Our SAR-IRSL protocol involved stimulation with IR diodes for 100 s at 50 °C and used the same thermal treatment prior to measuring the response to both regenerative and test doses (Huot and

Lamothe, 2003; Blair et al., 2005). The size of the test dose was 10 Gy in all experiments. Each measurement of the response to the test dose was followed by stimulation with the IR diodes for 40 s at 290 °C. Unless otherwise stated, the signals used for calculations were integrated over the first 1.2 s of stimulation minus a background evaluated from the last 10 s.

A representative SAR dose-response curve is shown in Fig. 12 for an aliquot of sample GLL-071806. The growth curve can be well represented by the sum of two single saturating exponential functions. In the example given, the corrected natural IRSL signal lies well below the laboratory saturation level, which is valid for all the investigated samples. Fig. 12 also illustrates the general behaviour of the samples in the SAR-IRSL protocol. Sensitivity changes occurring during the repeated SAR cycles are accurately corrected for, as is indicated by the ability to re-measure points on the dose-response curve (Fig. 12, open triangles). The dose-response curve passes close to the origin, demonstrating that recuperation is negligible (open circle in Fig. 12).

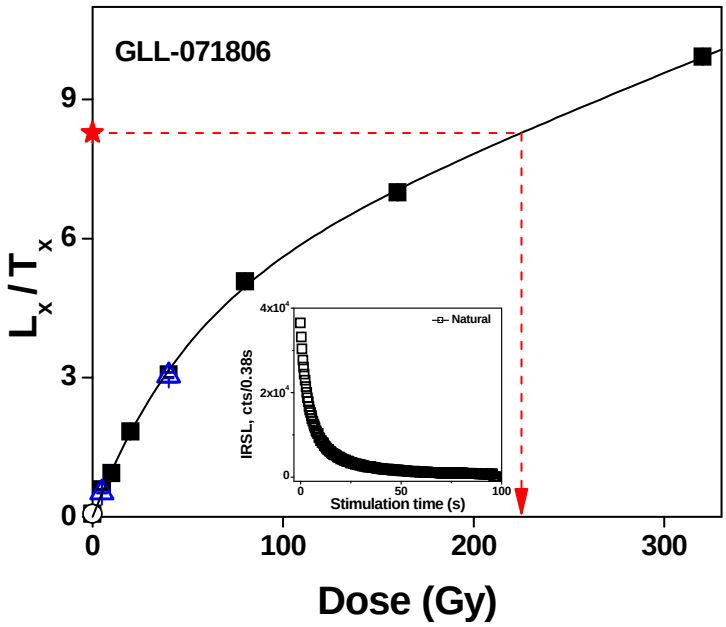

Figure 12: *Example of a SAR growth curve for one aliquot of sample GLL-071806. A preheat treatment of 60 s at 250 °C was employed. The natural L_x/T_x ratio is shown as a solid star; recycling points are shown as open triangles and the recuperation point as an open circle. The inset shows an example of a natural decay curve.*

Although recent studies on IRSL signals from sand-sized K-feldspar show that they are thermally stable up to a temperature of ~230 °C (e.g. Murray et al., 2009), it seems from the

above that the signals from the investigated polymineral-fine grains may have unstable, low temperature sources. Indeed, regenerated TL signals appear to have multiple low temperature components as shown in (Fig. 13).

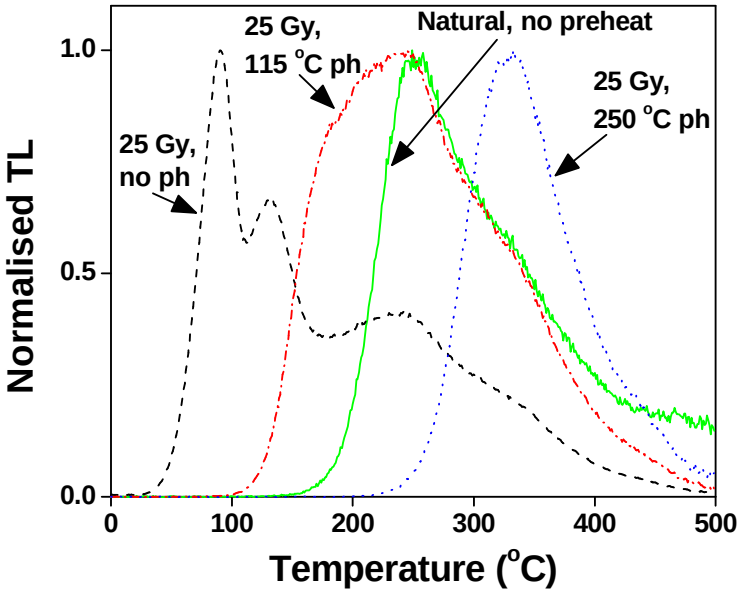

Figure 13: *TL signals normalised to the maximum intensity values. All signals were measured using one aliquot of sample GLL-071801: natural without preheating (solid line), 25 Gy regenerative dose without preheating (dashed line), 25 Gy regenerative dose followed by preheating at 115 °C for 60 s (dash-dot line) and 25 Gy regenerative dose followed by preheating at 250 °C for 60 s (dotted line).*

Combined IR/TL experiments indicate that low preheat treatments such as 115 °C are not able to completely remove all the thermally unstable components in the regenerated signal (see Fig. 14).

Furthermore pulse anneal data indicate that these persisting components appear to influence the thermal stability of the IRSL signal (Fig. 15). This contribution will not occur in the natural IRSL signals because of the short lifetime of the associated trap (see e.g. Strickertsson, 1988), but it will appear in the regenerated IRSL signals when no preheat is applied.

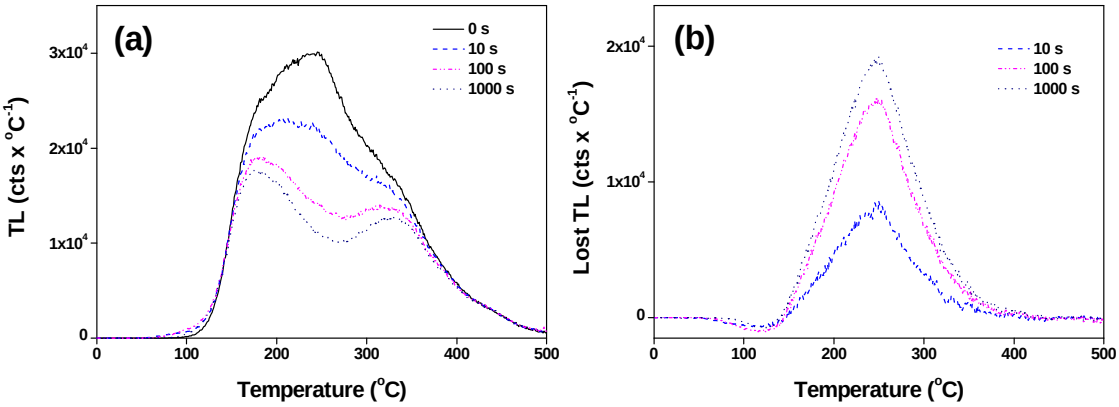

Figure 14: *(a) effect of prior IR on TL. An aliquot of polymineral fine grains of sample GLL-071801 was repeatedly heated (to 500 °C) and irradiated (25 Gy) until a stable TL signal was reached. The aliquot was then given a 25 Gy dose, preheated to 115 °C for 60 s and the TL signal measured after various times (0, 2, 4, 10, 40, 100, 200, 500 and 1000 s) of exposure to IR. The background was subtracted using a second TL signal measured immediately following first one. The measurements for 0, 4 and 40 s were repeated and yielded reproducible results. (b) TL lost as a result of IR stimulation. The curves were obtained by subtracting the TL curves after IR stimulation from the curved observed without stimulation.*

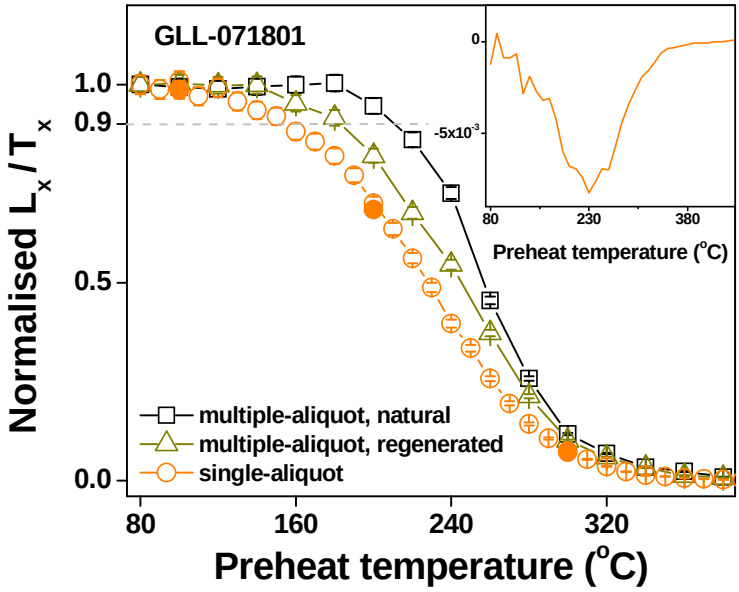

Figure 15: *Pulse anneal curves representing the variation of the sensitivity corrected IRSL signal with preheat temperature (see text for more details on the measurement procedure). The dashed line is meant as an eye guide and indicates a reduction of the IRSL signal by 10 %. The inset shows the first order derivative of the single-aliquot data.*

Therefore, the observed dependence of D_e on the preheat treatment applied (see Fig. 16) and, consequently, age underestimation when a low preheat is used (see Fig. 18) are caused by the low temperature contributions to the IRSL signal. This is further supported by the similar observations made using Serbian loess and the recent studies of Schmidt et al. (2010 and 2011) using Serbian and German loess, respectively.

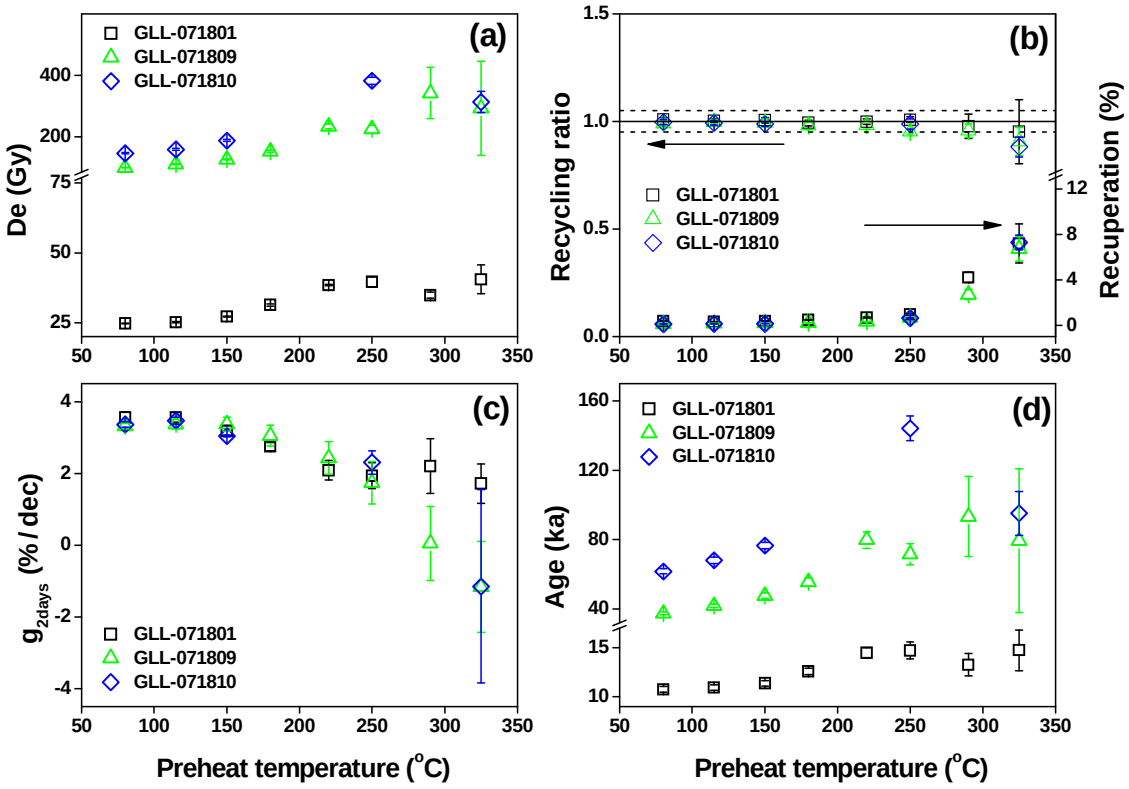

Figure 16: *Dependence on the preheat temperature of: (a) equivalent dose; (b) recycling ratio and recuperation corresponding to the aliquots measured in (a); (c) fading rate (g_{2days}-value) and (d) fading-corrected ages.*

The necessity of higher preheat treatments (e.g. 210-230 °C) to remove thermally unstable components has been suggested by several previous studies on TL and IRSL signals from loess or pure feldspars (see e.g. Wintle, 1985; Li, 1991 or Duller, 1994). A significant number of previous IRSL studies applied a preheat treatment to 250 °C for 60 s (see e.g. Huot and Lamothe, 2003; Buylaert et al., 2007).

However, our dose recovery experiments using a preheat to 250 °C for 60 s indicated the occurrence of significant initial sensitivity changes that the SAR protocol is unable to correct for (Fig. 17c).

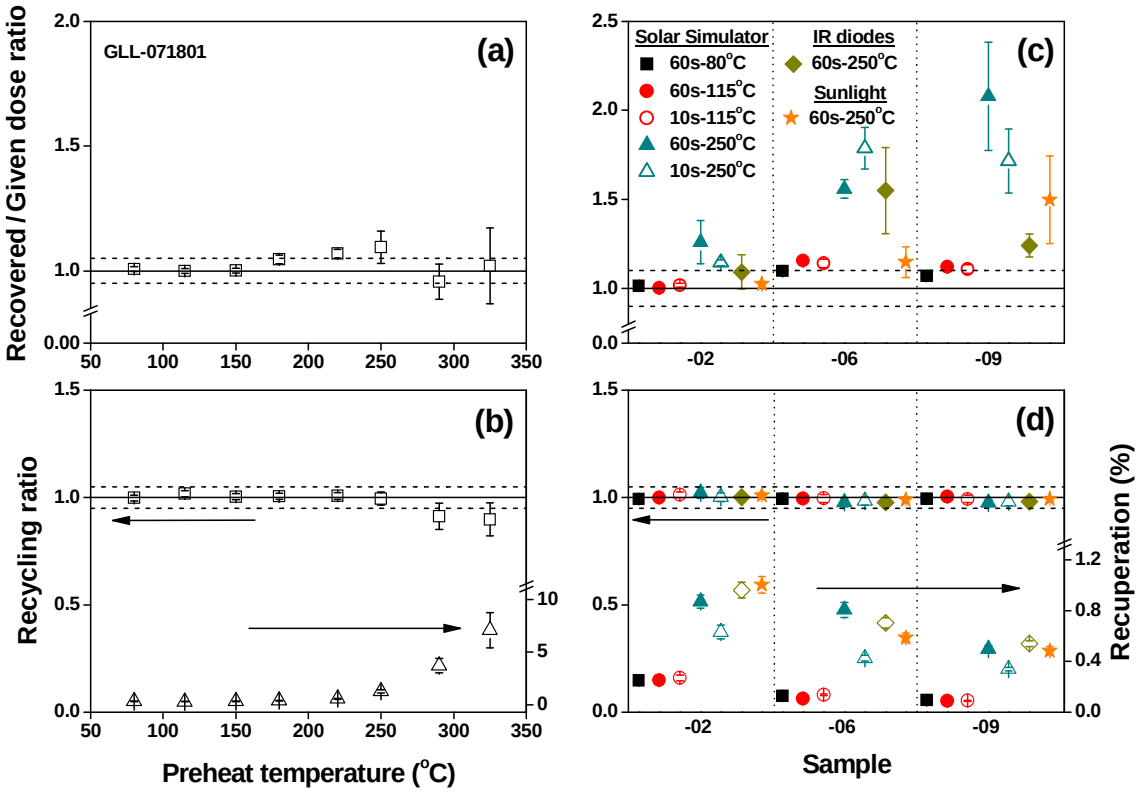

Figure 17: *(a) Dependence of dose recovery on preheat treatment for sample GLL-071801. (b) Recycling ratios and recuperation corresponding to the results shown in (a). (c) Results of the dose recovery test for samples GLL-071802, -06 and -09 using three preheat temperatures (80, 115 and 250 °C). (d) Recycling ratios and recuperation corresponding to the results shown in (c) respectively.*

The fading corrected age results obtained for the loess sequence at Mircea Vodă using this preheat treatment are in good agreement with previously reported quartz-OSL ages for samples collected in the uppermost loess unit L1 (Fig. 18). Furthermore, as the quartz-OSL age results corresponding to the samples collected from the deeper loess units were interpreted as age underestimates (Timar et al., 2010), the older IRSL age results obtained for these samples are not unexpected. Since the ability to recover a given dose was observed to depend on the bleaching

agent (see Fig. 18), it is considered that the age agreement obtained with the quartz-OSL results may not be a laboratory artifact.

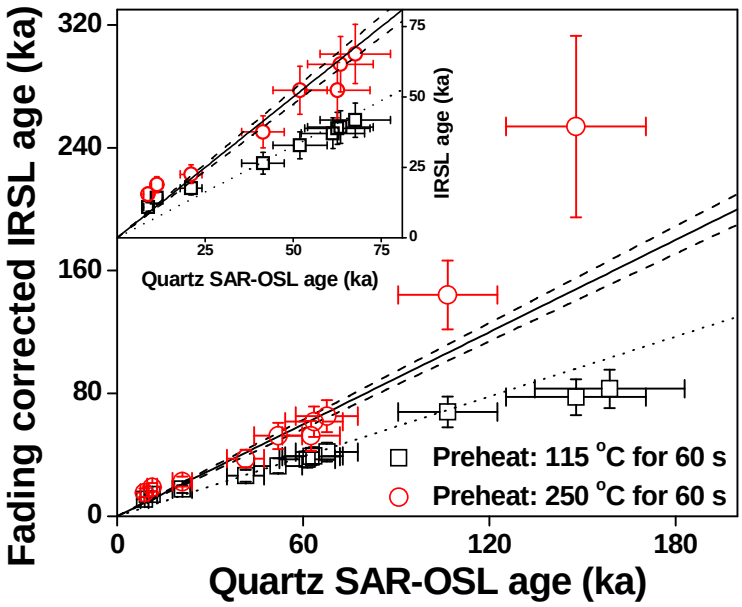

Figure 18: *Plot of fading corrected IRSL ages against fine silt quartz OSL ages obtained by Timar et al. (2010). Each data point is the average of minimum 3 aliquots measured for each sample. The inset shows the age results for the samples collected in the L1 loess unit.*

At this stage of our investigation, the chronology of the loess-palaeosol sequence near Mircea Vodă is not improved. Age results obtained from polymineral fine grains using conventional IRSL signals appear to be affected by thermal instability, initial sensitivity changes, and/or a combination of both phenomena. The initial age results proposed for the loess-palaeosol sequence at Belotinac should be interpreted with caution.

6. Testing the potential of elevated temperature post-IR IRSL signals for dating Romanian loess

In this study we test the potential of elevated temperature IRSL signals in a post-IR IRSL SAR protocol. The luminescence characteristics of IRSL and post-IR IRSL signals are documented using two preheat/stimulation temperature combinations in a SAR-based methodology.

Eight samples were investigated, considered as representative for the loess-palaeosol sequence near Mircea Vodă: five samples (GLL-071802, -03, -06, -07, -09) collected from the uppermost loess unit (L1), and three samples (GLL-071810, -12, -13) collected from the loess units below L2, L3 and L4, respectively.

All luminescence measurements were performed using a Risø TL/OSL-DA-15 reader. Infrared stimulation used IR LEDs emitting at 875 nm (Bøtter-Jensen et al. 2003) and IRSL signals were detected through a Schott BG39/Corning 7-59 filter combination passing light between 320 and 450 nm (Thomsen et al., 2008). Unless otherwise stated, a constant test dose of 10 Gy was given and a heating rate of 5 ^{o}C/s in a nitrogen atmosphere was employed.

The post-IR IRSL signals were documented using the modified SAR protocol given in Table 5, based on that developed for quartz by Murray and Wintle (2000). Two preheat - post-IR IR stimulation temperature combinations were used. In the first, a 60 s preheat treatment at 250 ^{o}C was followed by 100 s IR stimulation at 50 ^{o}C (IR_{50}) and a second 100 s stimulation at 225 ^{o}C (post-IR_{50} IR_{225}). The second post-IR IRSL protocol involved a 60 s preheat treatment at 325 ^{o}C and an elevated temperature IR stimulation at 300 ^{o}C (post-IR IR_{300}) following the IR_{50} stimulation.

	SAR protocol	Variable temperature	Measured IRSL
1.	Dose		
2.	Preheat, 60 s	250 or 325 ^{o}C	
3.	IRSL, 100 s at 50 ^{o}C		IR_{50}
4.	IRSL, 100 s $\rightarrow L_x$	225 or 300 ^{o}C	post-IR IR_T
5.	Test dose		
6.	Preheat, 60 s	250 or 325 ^{o}C	
7.	IRSL, 100 s at 50 ^{o}C		IR_{50}
8.	IRSL, 100 s $\rightarrow T_x$	225 or 300 ^{o}C	post-IR IR_T
9.	IRSL, 40 s	290 or 340 ^{o}C	
10.	Return to step 1		

Table 5: *The SAR protocol used for IRSL and post-IR IRSL measurements.*

Fig. 19 shows representative decay curves for both IR_{50} and post-IR IR_T signals recorded on an aliquot of sample GLL-071806, obtained using a single cycle of the protocol in Table 5.

The intensity of the IR_{50} signal after a preheat at 250 ^{o}C is slightly stronger than that of the post-IR IR_{225} (Fig. 19a); this is in contrast to the findings of Buylaert et al. (2009) who reported that for all their samples, the post-IR IR_{225} was ~ 2.5 times brighter than the prior IRSL at 50 ^{o}C. Nevertheless the two signals have similar decay rates (see Fig. 19a-inset). On the other hand, the intensity of the post-IR IR_{300} signal is significantly stronger than the intensity of the corresponding IR_{50} signal measured after a preheat at 325 ^{o}C (Fig. 19b). The latter is also observed to have a slower decay rate and to have a significant background level relative to its initial intensity (see Fig. 19b-inset). This is due to the weak signal remaining after the thermal erosion caused by preheating at 325 ^{o}C for 100 s.

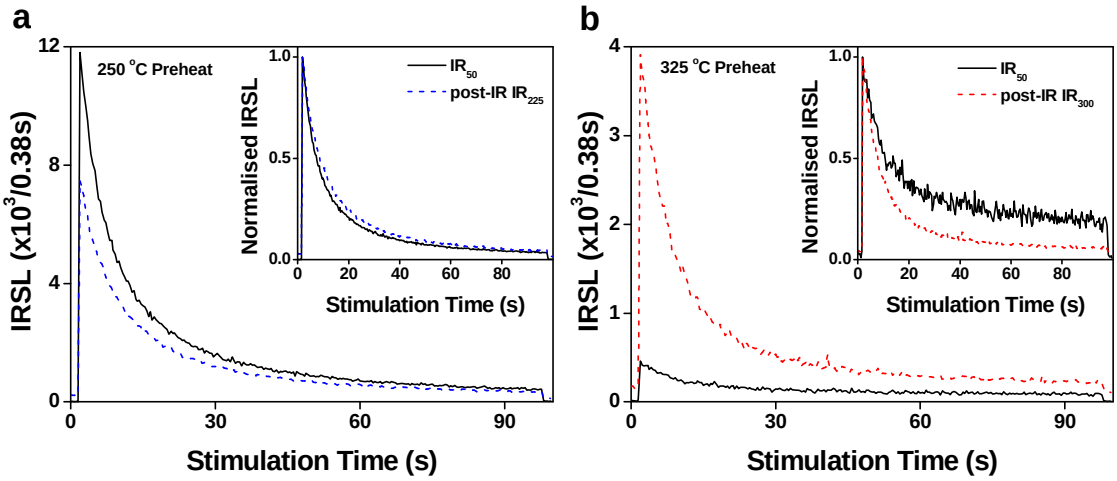

Figure 19: *Representative decay curves for (a) IR_{50} and post-IR IR_{225} (measured after an initial preheat at 250 ^{o}C) and (b) IR_{50} and post-IR IR_{300} (measured after an initial preheat at 325 ^{o}C). The insets in (a) and (b) show the same signals but normalized to their maximum intensity.*

The performances and dating potential of two post-IR IR_T protocols are evaluated. The post-IR IR_{225} signal is observed to successfully pass the SAR performance tests in terms of recycling ratio, recuperation and dose recovery (see Table 6). Similarly with the observations of Buylaert et al. (2009) and Thiel et al. (2010), fading rates measured for this signal are significantly smaller than the values obtained for the corresponding IR_{50} signal (see Table 7). Therefore, the post-IR IR_{225} signal appears be suitable for obtaining reliable age results for the investigated samples. Furthermore, both natural and laboratory induced signals were observed to correspond to the saturating region of the dose response curve (Fig. 20). This indicates that the observed fading is probably artificially induced, excluding the need of fading correction. A

similar observation was recently reported by Thiel et al. (2011) using a post-IR IR_T signal stimulated at 290 ^oC.

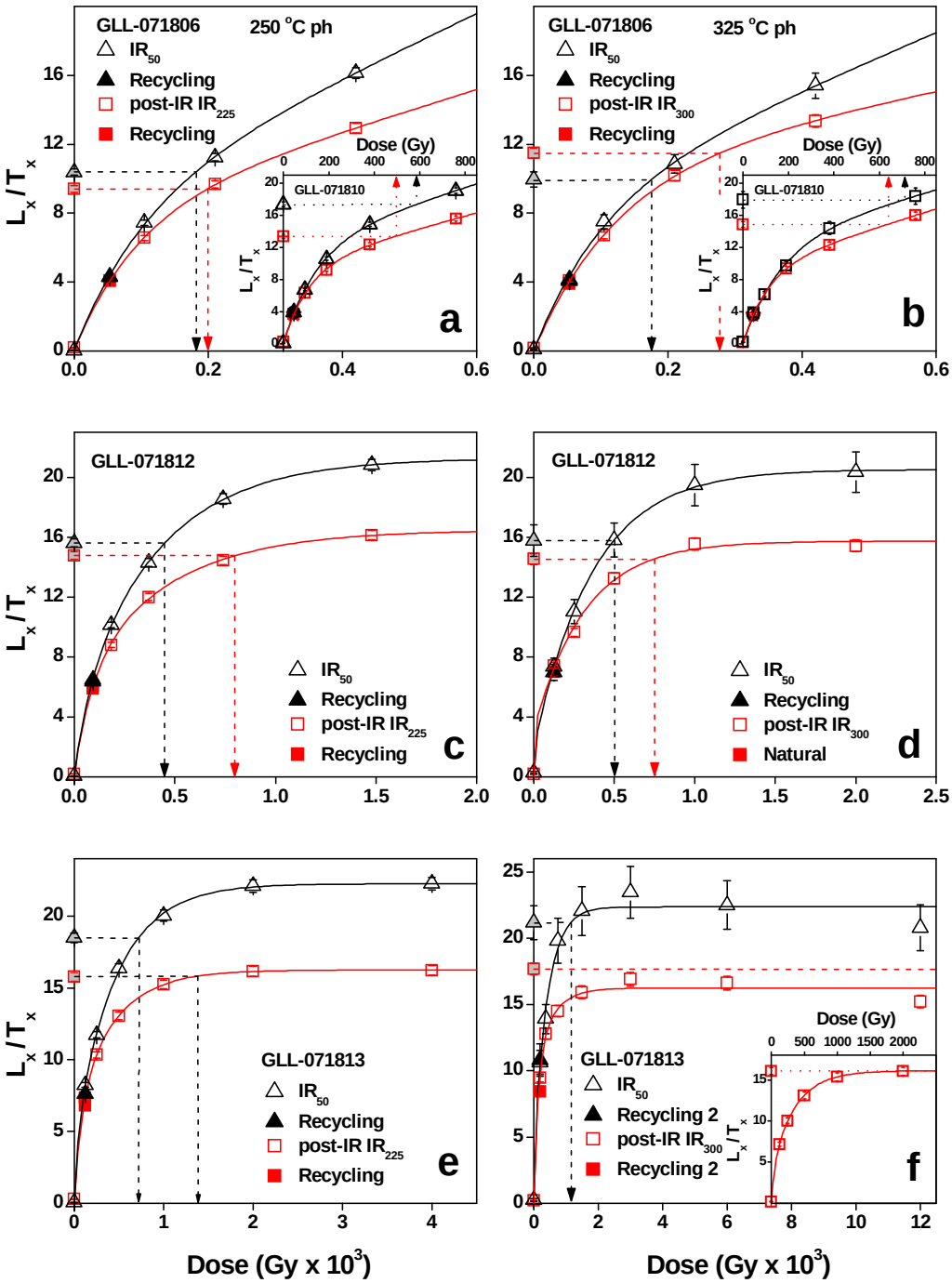

Figure 20: *Examples of dose response curves of signals obtained using the two SAR protocols: IR_{50} and post-IR IR_{225} (a,c,e); IR_{50} and post-IR IR_{300} (b,d,f). The signals were measured using aliquots of samples collected from different loess units: GLL-071806 (a,b); GLL-071810 (insets in a and b); GLL-071812 (c,d) and GLL-071813 (e,f).*

Loess Unit	Sample	Depth (m)	IRSL signal	Recycling ratio	Given dose (Gy)	Recovered/ given dose	Residual dose (Gy)
L1	**GLL-071802**	1.05	**post-IR IR_{225}**	0.99 ± 0.02	50	0.99 ± 0.03	3.8 ± 0.3
	n=3		**IR_{50}**	1.01 ± 0.02		1.06 ± 0.02	1.6 ± 0.1
			post-IR IR_{300}	1.02 ± 0.03	50	0.95 ± 0.08	11.3 ± 0.3
			IR_{50}	0.96 ± 0.09		1.08 ± 0.16	5.5 ± 0.5
	GLL-071803	1.30	**post-IR IR_{225}**	0.98 ± 0.01			
	n=6		**IR_{50}**	1.01 ± 0.01			
			post-IR IR_{300}	0.99 ± 0.02			
			IR_{50}	1.01 ± 0.05			
	GLL-071806	2.80	**post-IR IR_{225}**	0.96 ± 0.01	210	1.00 ± 0.05	9.9 ± 0.3
	n=6		**IR_{50}**	0.96 ± 0.01		1.43 ± 0.25	2.9 ± 0.1
			post-IR IR_{300}	0.93 ± 0.03	210	1.03 ± 0.05	23.8 ± 1.0
			IR_{50}	0.96 ± 0.07		0.80 ± 0.11	10.2 ± 1.6
	GLL-071807	3.75	**post-IR IR_{225}**	0.97 ± 0.01			
	n=6		**IR_{50}**	0.97 ± 0.01			
			post-IR IR_{300}	0.96 ± 0.02			
			IR_{50}	0.95 ± 0.05			
	GLL-071809	5	**post-IR IR_{225}**	0.97 ± 0.02	260	0.99 ± 0.03	10.1 ± 0.3
	n=3		**IR_{50}**	1.01 ± 0.02		1.34 ± 0.03	2.9 ± 0.1
			post-IR IR_{300}	1.01 ± 0.03	230	0.95 ± 0.04	20.5 ± 0.7
			IR_{50}	0.91 ± 0.06		0.85 ± 0.08	11.9 ± 3.9
L2	**GLL-071810**	8	**post-IR IR_{225}**	0.98 ± 0.02	460	1.03 ± 0.04	12.7 ± 1.3
	n=3		**IR_{50}**	0.98 ± 0.02		1.79 ± 0.20	3.4 ± 0.3
			post-IR IR_{300}	0.96 ± 0.03	640	1.10 ± 0.11	30.1 ± 0.8
			IR_{50}	0.90 ± 0.11		1.17 ± 0.38	13.3 ± 1.1
L3	**GLL-071812**	15	**post-IR IR_{225}**	0.97 ± 0.01	800	1.31 ± 0.20	14.1 ± 0.7
	n=6		**IR_{50}**	0.97 ± 0.01		1.87 ± 0.11	3.9 ± 0.2
			post-IR IR_{300}	0.97 ± 0.03	1300	X	30.2 ± 1.4
			IR_{50}	0.90 ± 0.05		0.79 ± 0.13	11.8 ± 1.4
L4	**GLL-071813**	18	**post-IR IR_{225}**	0.96 ± 0.01	1200	2.04 ± 0.23	17.0 ± 0.4
	n=6		**IR_{50}**	0.95 ± 0.01		2.45 ± 0.41	4.3 ± 0.2
			post-IR IR_{300}	0.94 ± 0.02	1600	X	33.2 ± 1.1
			IR_{50}	0.86 ± 0.05		1.49 ± 0.53	13 ± 0.9

Table 6: *Summary of recycling ratio, dose recovery and residual doses.*

Sample GLL-	Depth (m)	Dose rate (Gy/ka)	IRSL signal	D_e (Gy)	$Age_{uncorr.}$ (ka)	g_{2days} (%/decade)	$Age_{corrr.}$ (ka)	σ_r (%)	σ_{sys} (%)
071802	1.05	3.22 ± 0.06	**post-IR IR_{225}**	60 ± 1 (n=3)	**19 ± 3**	0.6 ± 0.2	19 ± 3	2	14
			IR_{50}	55 ± 5	17 ± 3	2.1 ± 0.1	**20 ± 4**	10	
			post-IR IR_{300}	58 ± 3	**18 ± 3**	0.6 ± 0.4	19 ± 3	6	
			IR_{50}	40 ± 3	**12 ± 2**	-2.1 ± 0.5		7	
071803	1.30	3.46 ± 0.05	**post-IR IR_{225}**	80 ± 1 (n=6)	**23 ± 3**	1.3 ± 0.2	26 ± 4	2	14
			IR_{50}	76 ± 4	22 ± 3	2.9 ± 0.4	**29 ± 5**	8	
			post-IR IR_{300}	86 ± 5	**25 ± 4**	0.6 ± 0.4	26 ± 4	6	
			IR_{50}	66 ± 4	**19 ± 3**	0.9 ± 0.9		6	
071806	2.80	3.50 ± 0.05	**post-IR IR_{225}**	212 ± 5 (n=6)	**60 ± 9**	1.2 ± 0.2	67 ± 10	3	15
			IR_{50}	175 ± 5	50 ± 7	2.8 ± 0.2	**65 ± 10**	4	
			post-IR IR_{300}	285 ± 11	**74 ± 11**	-0.4 ± 0.5	74 ± 11	5	
			IR_{50}	156 ± 9	**45 ± 7**	-3.1 ± 1.5		6	
071807	3.75	3.58 ± 0.05	**post-IR IR_{225}**	232 ± 7 (n=6)	**65 ± 10**	1.1 ± 0.2	71 ± 11	4	15
			IR_{50}	202 ± 11	56 ± 9	2.5 ± 0.1	**71 ± 11**	6	
			post-IR IR_{300}	261 ± 26	**73 ± 13**	1.1 ± 0.5	80 ± 15	10	
			IR_{50}	182 ± 22	**51 ± 10**	-1.8 ± 0.6		12	
071809	5	3.69 ± 0.04	**post-IR IR_{225}**	257 ± 16 (n=3)	**70 ± 11**	0.8 ± 0.1	75 ± 12	6	15
			IR_{50}	290 ± 70	79 ± 22	2.6 ± 0.2	**101 ± 29**	24	
			post-IR IR_{300}	231 ± 9	**63 ± 9**	0.6 ± 0.1	66 ± 10	4	
			IR_{50}	156 ± 19	**42 ± 8**	-2.1 ± 1.7		12	
071810	8	3.30 ± 0.05	**post-IR IR_{225}**	454 ± 24 (n=3)	**138 ± 22**	1.3 ± 0.1	156 ± 24	5	15
			IR_{50}	433 ± 80	131 ± 31	3.0 ± 0.2	**176 ± 42**	19	
			post-IR IR_{300}	640 ± 27	**194 ± 30**	1.5 ± 0.7	224 ± 38	5	
			IR_{50}	529 ± 102	**161 ± 39**	-0.5 ± 0.8		19	
071812	15	3.29 ± 0.06	**post-IR IR_{225}**	805 ± 65 (n=6)	**245 ± 42**	1.0 ± 0.2	269 ± 46	8	15
			IR_{50}	517 ± 29	157 ± 25	2.4 ± 0.2	**199 ± 32**	6	
			post-IR IR_{300}	1321 ± 231	**401 ± 92**	0.7 ± 0.4	429 ± 100	18	
			IR_{50}	463 ± 61	**141 ± 28**	-1.3 ± 0.9		13	
071813	18	3.30 ± 0.04	**post-IR IR_{225}**	1188 ± 155 (n=6)	**360 ± 71**	1.5 ± 0.3	415 ± 83	13	15
			IR_{50}	812 ± 85 (n=6)	246 ± 45	2.9 ± 0.2	**328 ± 60**	11	
			post-IR IR_{300}	1604 ± 162 (n=3)	**486 ± 88**	-0.3 ± 0.4	491 ± 89	10	
			IR_{50}	796 ± 66 (n=5)	**241 ± 41**	-0.5 ± 0.4		8	

Table 7: *Summary of calculated dose rates, equivalent doses (D_e), uncorrected ages, fading rates (g_{2days}), fading-corrected ages, random (σ_r) and systematic (σ_s) uncertainties.*

For samples collected from the loess units L1 and L2, the post-IR IR_{300} signal seems to have a similar dating potential as the post-IR IR_{225} (Table 6). In addition, the fading rates measured for this signal appear even lower than for the post-IR IR_{225} signal (Table 7). However, for some of the measured aliquots of the lowermost sample (GLL-071813), the natural signal appears to fall above the saturation level of the dose response curve (Fig. 20f). The same behaviour was observed in dose recovery measurements for samples GLL-071812 and -13. It appears that artificial irradiation with large doses lead to initial sensitivity changes that the SAR protocol is unable to correct for. Several studies report a similar behaviour for quartz OSL signals (Yoshida et al., 2000; Bailey et al., 2005). We have no knowledge of a similar observation in IRSL dating studies available in the literature. Further investigations are necessary in order to document this anomalous behaviour and therefore, we refrain from further discussing the age results obtained using the post-IR IR_{300} signal.

In Fig. 21 the uncorrected post-IR IR_{225} ages, are plotted together with the two types OSL ages obtained by Timar et al. (2010 and 2011) using silt-sized (4-11µm) and fine sandy (63-90 µm) quartz. In addition the magnetic time-depth model proposed by Timar et al. (2010) is shown.

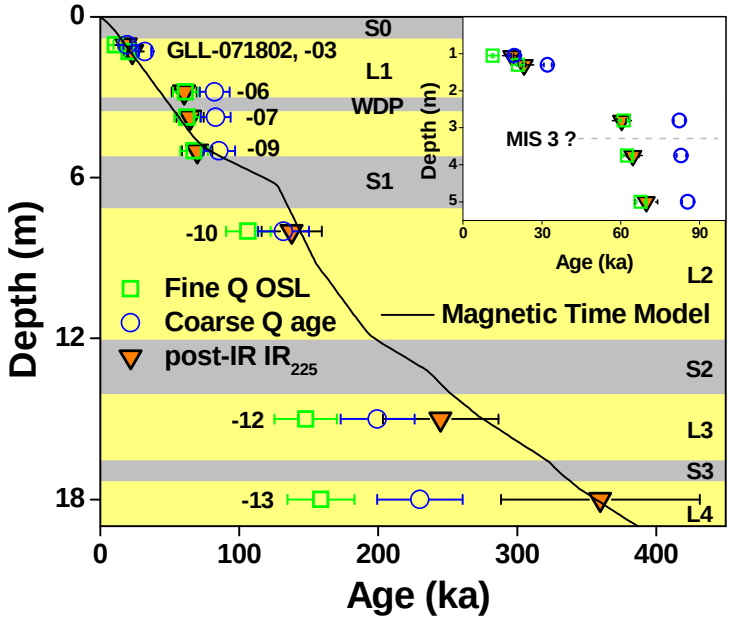

Figure 21: *Summary of uncorrected post-IR IR_{225} ages versus depth. The silt- and sand-sized quartz OSL ages and palaeomagnetic time-depth model (Timar et al., 2010 and 2011) are shown as well. The error bars 1σ total uncertainty. The inset shows the results (1σ random uncertainty) obtained for the uppermost loess unit L1.*

The post-IR IR_{225} age results obtained for the samples in L1 and L2 are generally consistent with the silt-sized quartz OSL ages, whereas for the samples collected from L3 and L4 the ages based on both types of quartz grain-size are increasingly underestimated. However, the ages based on the coarser quartz fraction (63-90 µm) appear consistent within one and two standard errors with the post-IR IR_{225} ages for samples GLL-071812 and -13 respectively. Nevertheless, considering the possible limitations of quartz-based SAR-OSL dating of older samples (Murray et al., 2007), the observed underestimation of quartz-based ages is not surprising. For the sample in L3 the post-IR IR_{225} age is in excellent agreement with the age obtained by Balescu et al. (2010) for a sample collected at the same depth. This independent result, together with the age suggested by the magnetic time-depth model (Timar et al., 2010) support older depositional ages for the material collected at this depth than the obtained age results based on 63-90 µm quartz fraction (Timar et al. 2011).

It is considered that the uncorrected post-IR IR_{225} age results are reliable and may be used as an independent age control for solving the quartz-based discrepant chronology observed by Timar et al. (2011). For samples in the loess unit L1, the agreement between the post-IR IR_{225} ages and the silt-sized quartz OSL ages is consistent with the previously obtained agreement between IRSL ages (using IR stimulation at 125 ^{o}C and UV detection; Vasiliniuc et al., submitted) and the same quartz-based ages of Timar et al. (2010). Thus, the post-IR IR_{225} ages provide an additional support of the silt-sized quartz OSL chronology over the last interglacial-glacial period. These datasets allocate the formation of the weak palaeosol intercalated in L1 and three uppermost palaeosols in the section (S1, S2 and S3; see Timar et al., 2010) during MIS 3, 5, 7 and 9 respectively. In addition, the change in sedimentation rate observed by Timar et al. (2010) to coincide with the transition from MIS 4 to MIS 3 is considered reliable/accurate.

Summary

One of the aims of this PhD project was to extend the quartz OSL investigations in order to see whether the discrepant behaviour observed at Mircea Vodă (Timar et al., 2010 and 2011) is a general feature of loess in the region. Our study of quartz extracted from the loess sequence at Mostiştea used the same methodology as that used in the studies of Timar et al. (2010 and 2011). The signals selected for analysis from both grain-size fractions of quartz appear very

similar to the ones investigated for samples at Mircea Vodă. The dominance of the fast component in the OSL signals is indicated by the decay shape of the CW-OSL signal and by LM-OSL comparisons with calibration quartz. Furthermore, both quartz fractions passed the procedural tests of the single-aliquot regenerative-dose (SAR) protocol (i.e. recycling ratio, recuperation and dose recovery) indicating that the protocol should provide reliable D_e values. However, the age results obtained for the two fractions are generally inconsistent; similarly to the results obtained by Timar et al. (2011) at Mircea Vodă (i.e. the sand-sized quartz ages are generally older than the silt-sized quartz ages). The age discrepancy resides in the D_e values obtained for the two quartz fractions.

High resolution anneal experiments exclude a possible contribution from a thermally unstable component to the OSL signals from both fractions. Furthermore, the possibility of incomplete bleaching of the OSL signal in the sand-sized quartz does not seem to hold as residual doses up to more than 100 Gy are needed to compensate for the difference in D_e.

The only difference between the two quartz fractions is in the saturation characteristics of the dose response curves. For both fractions the dose response curves are best fitted with the sum of two saturating exponential terms. Moreover, for each of the quartz fractions the saturation characteristics are independent of the age or the sample. However, the characteristic saturation dose values for the two exponential functions that fit the dose-response curves are significantly higher for the silt-sized fraction than for the sand-sized fraction. Since the equivalent doses of our samples (at least for the coarse grains) are obtained by interpolating on a region of the dose response curve where the first exponential component is already in saturation, the reliability of using this region of the dose response curve for quartz SAR-OSL dating is questionable.

The main objective of this work was to use luminescence signals from feldspars in order to establish an accurate chronology for Romanian loess. Three different measurement procedures were applied to polymineral fine grains extracted from the loess sequence at Mircea Vodă: double-SAR, conventional IRSL and post-IR IRSL. These are all based on the SAR protocol, the most robust measurement routine available at the moment.

The two signals obtained using the double-SAR protocol, IRSL and post-IR OSL, successfully passed laboratory tests, indicating that the protocol is suitable for D_e determination for both signals. However, the optical separation of the contributions from quartz and feldspar does not appear to be total. The IRSL and post-IR OSL signals exhibit anomalous fading, and the

ages derived from these signals are therefore dependent on the fading correction model. Further improvements in the protocol may be achieved by finding the optimum measurement conditions in order to have a better separation of the two contributions. Nevertheless, a general agreement was obtained between the fading corrected age results obtained with both IRSL and post-IR OSL signals and the silt-sized quartz OSL ages obtained by Timar et al. (2010). However, since the quartz OSL ages were interpreted as underestimates for material deposited before the last interglacial period, this agreement is considered valid only for samples collected from the uppermost loess unit L1. The chronology of the loess sequence near Mircea Vodă could not be extended beyond the last glacial period due to limitations of the fading correction method.

The further application of conventional IRSL procedure (IR stimulation at 50 ^{o}C) to date polymineral fine grains extracted from Romanian loess was rather problematic. Dose recovery experiments indicate that the SAR protocol is unable to recover a known given dose when high temperature preheats are employed. This corroborated the need to use signals obtained after low preheat treatments. However, age results obtained using a preheat at 115 ^{o}C for 60 s were significantly underestimating the previously obtained silt-sized quartz OSL ages. Pulse anneal and combined IR/TL experiments indicated that the underestimation is caused by a thermally unstable contribution to the regenerated signals.

It is considered that the conventional IRSL approach is not able to provide accurate depositional ages for Romanian loess due to initial sensitivity changes that occur when a high preheat treatment is applied and/or to contributions from thermally unstable components observed after low preheats. Furthermore, initial results obtained for polymineral fine grains extracted from the loess sequence at Belotinac (Serbia) indicate that this problem may not be specific to Romanian loess.

The third procedure that we applied is based on the recently proposed post-IR IRSL protocol. The two post-IR IR_T signals were documented using a modified SAR protocol. The post-IR IR_{225} signal is observed to successfully pass the SAR performance tests in terms of recycling ratio, recuperation and dose recovery. Furthermore, both natural and regenerated signals were observed to correspond to the saturating region of the dose-response curve, indicating that the small fading rate determined for this signal is probably an artefact of the measurement procedure.

The post-IR IR_{300} signal appears to have similar results in the SAR performance tests, and an even smaller fading rate than the post-IR IR_{225} signal. However this signal appears to suffer from dose dependent initial sensitivity changes that cause the observation of both natural and laboratory induced signals above the saturation level of the dose response curve. Since this anomalous behaviour is not understood, we are questioning the accuracy of the post-IR IR_{300} ages.

The ages obtained from the post-IR IR_{225} signal are in agreement with the OSL ages for silt-sized quartz for samples collected from the uppermost loess unit L1 and with independent age control for samples collected deeper down the section (in L2, L3 and L4).

The two IRSL signals stimulated at 50 ^{o}C (after preheats at either 250 °C or 325 °C), appear unsuitable for dating. On the one hand the signal obtained after preheating to 250 ^{o}C has poor performance in the dose recovery test, as expected from our previous conventional IRSL investigations. On the other hand, the thermal erosion due to the high preheat at 325 ^{o}C leads to inappropriate fading measurement.

Conclusions

Methodological

The results from the quartz-based OSL study at Mostiştea indicate that the age discrepancy observed between two grain sizes of quartz may be characteristic for loess deposits in SE Romania. The presence of an additional function, besides a single saturating exponential, in the dose response curves constructed for both types of quartz grains, may indicate that there are still unknown processess that influence the characteristics of the signals used for age determination. Therefore, these results suggested that the reliability of the age results obtained from signals with similar saturation characteristics of the dose response curve should be regarded with caution.

The experiments using polymineral fine grains extracted from the loess sequence near Mircea Vodă allowed evaluation of the potential of IRSL signal to establish an accurate chronology for this sequence.

The use of the double SAR protocol appears to be a suitable alternative for dating Romanian loess, avoiding the need to isolate pure quartz using chemical procedures. Although the IRSL and post-IR OSL signals exhibit anomalous fading, and the ages derived from these signals are therefore dependent on the fading correction model, an agreement between ages obtained using feldspar (IRSL), quartz (OSL) and/or mixed (post-IR OSL) signals increases confidence in the dating results. However, the chronology of the loess sequence near Mircea Vodă could not be extended beyond the last glacial period due to limitations of the fading correction method.

The further application of conventional IRSL procedure to date polymineral fine grains extracted from Romanian loess was rather problematic. Although previous studies on feldspars indicate that preheating may not be necessary in order to isolate a thermally stable signal, our work shows that this is not valid for the samples investigated. Moreover, our experiments show that the use of a high preheat treatment is hampered by initial sensitivity changes. Initial results for Serbian loess indicate that the problem may be more general.

The recently developed post-IR IRSL protocol was also tested using polymineral fine grains. Our observations support the previous studies reporting that the post-IR IR_T signals obtained using an elevated stimulation temperature may not suffer from fading. Methodologically, the post-IR IR_{225} signal is considered the best alternative to date these samples as it passes all procedural checks. This is confirmed by the agreement between the uncorrected post-IR IR_{225} age results and the OSL ages for silt-sized quartz for samples collected from the uppermost loess unit L1 and with independent age control for samples collected deeper down the section (in L2, L3 and L4). The post-IR IR_{300}, however, appears to suffer from dose dependent initial sensitivity changes that hamper its use for the oldest samples investigated.

It is therefore considered that the post-IR IR_{225} signal may provide the necessary insights to clarify the age discrepancy observed in the quartz OSL studies. The use of this signal for the samples collected at Mostiştea would throw more light onto this problem.

Chronological

The age discrepancy between the silt- and sand-sized quartz grains investigated at Mostiştea appears larger than the one obtained for the loess section near Mircea Vodă.

Using alternative procedures to investigate luminescence signals from feldspars, such as the double-SAR and post-IR IRSL protocol, an independent age control was obtained for the loess sequence at Mircea Vodă. The feldspar-based age results obtained using polymineral fine grains agree with the silt-sized chronology for samples collected from the uppermost loess unit L1. This agreement increases the confidence in the reliability of silt-sized quartz as a dosimeter for the last glacial period. It further confirms that the uppermost palaeosol unit S1 has formed during MIS 5 and that the change in sedimentation rate observed for the L1 unit corresponds to the formation of a weakly developed palaeosol during MIS 3. Furthermore, the post-IR IR_{225} ages correlate the formation of the lower palaeosols, S2 and S3, during MIS 7 and 9 respectively.

Our work brings further evidence that the S1 and S2 units can no longer be thought of as interstadial soils that developed during the Last Glacial, indicating that the chronostratigraphical framework proposed by Conea (1969) is not accurate. Furthermore, the obtained age results are further confirming the potential of luminescence dating to detect variations in dust transport and deposition and also to assess the reliability of proxy-based methods.

A further direction of study would be to extend the post-IR IRSL investigations to other representative loess sequences in Romania. The promising results obtained using these signals may allow an extended chronological correlation of loess deposition in this region.

Selected References

Adamiec G and Aitken M, 1998. Dose-rate conversion factors: update. *Ancient TL* 16: 37-50.

Aitken, M.J., 1985. Thermoluminescence Dating. Academic Press, London.

Balescu, S., Lamothe, M., Mercier, N., Huot, S., Balteanu, D., Billiard, A., Hus, J., 2003. Luminescence chronology of Pleistocene loess deposits from Romania: testing methods of age correction for anomalous fading in alkali feldspars. Quaternary Science Reviews 22, 967-973.

Balescu, S., Lamothe, M., Panaiotu, C., Panaiotu, C., 2010. La chronologie IRSL des séquences loessiques de l'Est de La Roumanie. Quaternaire 21, 115-126.

Bailey, R.M., Armitage, S.J., Stokes, S., 2005. An investigation of pulsed-irradiation regeneration of quartz OSL and its implications for the precision and accuracy of optical dating. Radiation Measurements 39, 347-359.

Banerjee, D., Murray, A.S., Bøtter-Jensen, L., Lang, A., 2001. Equivalent dose estimation using a single aliquot of polymineral fine grains. Radiation Measurements 33, 73-94.

Blair, M.W., Yukihara, E.G., McKeever, S.W.S., 2005. Experiences with single-aliquot OSL procedures using coarse-grain feldspars. Radiation Measurements 37, 361-374.

Bøtter-Jensen, L., Murray, A.S., 1999. Developments in optically stimulated luminescence techniques for dating and retrospective dosimetry. Radiation Protection Dosimetry 84, 307-315.

Bøtter-Jensen, L., McKeever, S.W.S., Wintle, A.G., 2003. Optically Stimulated Luminescence Dosimetry. Elsevier Science, The Netherlands.

Buggle, B., Glaser, B., Zöller, L., Hambach, U., Marković, S., Glaser, I., Gerasimenko, N., 2008. Geochemical characterisation and origin of Southeastern and Eastern European loesses (Serbia, Romania, Ukraine). Quaternary Science Reviews 27, 1058-1075.

Buylaert, J.-P.,Vandenberghe, D., Murray, A.S., Huot, S., De Corte, F., Van den haute, P., 2007. Luminescence dating of old (>70 ka) Chinese loess: a comparison of single-aliquot OSL and IRSL techniques. Quaternary Geochr. 2, 9-14

Buylaert, J.P, Murray, A.S., Thomsen, K.J., Jain, M., 2009. Testing the potential of an elevated temperature IRSL signal from K-feldspar. Radiation Measurements 44, 560-565.

Buylaert, J.P., Huot, S., Murray, A.S., van den Haute, P., 2011. Infrared stimulated luminescence dating of an Eemian (MIS 5e) site in Denmark using K-feldspar. Boreas 40, 46-56, doi: 10.1111/j.1502-3885.2010.00156.x.

Codrea, V., 1998. Geologia Cuaternarului. Noțiuni de bază. (Quaternary Geology. Basic notions) Babeş-Bolyai University, Cluj Napoca.

Conea A, 1969. Profils de loess en Roumanie. La stratigraphy des loess d'Europe. In: Fink J, ed., *Bulletin de l'Association Française pour l'étude du Quaternaire*. Suppl. INQUA: 127-134.
Conea A, 1970. *Formațiuni Cuaternare în Dobrogea (loessuri şi paleosoluri)* (Quaternary units

Duller, G.A.T., Bøtter-Jensen, L., 1993. Luminescence from potassium feldspars stimulated by infrared and green light. Radiat. Prot. Dosimetry 47, 683–688.

Duller, G.A.T., 1997. Behavioural studies of stimulated luminescence from feldspars. Radiation Measurements 27, 663-694.

Duller G.A.T., Wintle, A.G., 1991. On infrared stimulated luminescence at elevated temperatures. Nuclear Tracks and Radiation Measurements 18, 379-384.

Frechen, M., Oches, E.A., Kohfeld, K.E., 2003. Loess in Europe – mass accumulation rates during the Last Glacial Period. Quaternary Science Reviews 22, 1835-1857.

Godfrey-Smith, D.I., Huntley, D.J., Chen, W.-H., 1988. Optical dating studies of quartz and feldspar sediment extracts. Quaternary Science Reviews 7, 373-380.

Haase, D., Fink. J., Haase, G., Ruske, R., Pecsi M., Richter, H., Altermann, M., Jager, K.-D., 2007. Loess in Europe – its spacial distribution based on a European Loess Map, scale 1:2,500,000. Quaternary Science Reviews 26, 1301-1312.

Huntley, D.J., Lamothe, M., 2001. Ubiquity of anomalous fading in K-feldspars and the measurement and correction for it in optical dating. Canadian Journal of Earth Sciences 38, 1093-1106.

Huntley, D.J., Lian, O.B., 2006. Some observations on tunnelling of trapped electrons in feldspars and their implications for optical dating. Quaternary Science Reviews 25, 2503-2512.

Huot, S., Lamothe, M., 2003. Variability of infrared stimulated luminescence properties from fractured feldspar grains. Radiation Measurements 37, 499-503.

Jain, M., Singhvi, A.K., 2001. Limits to depletion of blue-green light stimulated luminescence in feldspars: implications for quartz dating. Radiation Measurements 33, 883-892.

Krbetschek M.R., Götze J., Dietrich, A., Trautmann, T., 1997. Spectral information from minerals relevant for luminescence dating. Radiation Measurements 27, 695-748.

Kukla, G.J, Bender, M.L., Beaulieu, J-L., 2002. Last interglacial climates. Quaternary Research 58, 2-13.

Li, B., Li, S.-H., 2011. Thermal stability of infrared stimulated luminescence of sedimentary K-feldspar. Radiation Measurements 46, 29-36.
xLi, S.-H., Wintle, A.G., 1992. A global view of luminescence signals from loess. Quaternary Sci. Rev. 11, 133-137.

Maher, B.A., 2011. The magnetic properties of Quaternary aeolian dusts and sediments, and their palaeoclimatic significance. Aeolian Research 3, 87-144.

Marković, S.B., Hambach, U., Catto, N., Jovanovic M., Buggle, B., Machalett, B., Zöller, L., Glaser, B., Frechen, M., 2009. Middle and Late Pleistocene loess sequences at Batajnica, Vojvodina, Serbia. Quaternary International 198, 255-266.

Mejdahl M, 1979. Thermoluminescence dating : beta dose attenuation in quartz grains. *Archaeometry* 21: 61-67.

Murray, A.S., Wintle, A.G., 2000. Luminescence dating of quartz using an improved single-aliquot regenerative-dose protocol. Radiation Measurements 32, 57-73.

Murray, A.S., Olley, J.M., 2002. Precision and accuracy in the optically stimulated luminescence dating of sedimentary quartz: a status review. Geochronometria 21, 1-16.

Murray, A.S., Buylaert, J.-P., Thomsen, K.J., Jain, M., 2009. The effect of preheating on the IRSL signal from feldspar. Radiat. Meas. 44, 554-559.

Necula C and Panaiotu C, 2008. Application of dynamic programming to the dating of a loess-palaesol sequence. *Romanian Reports in Physics* 60: 157-171.

Panaiotu CG, Panaiotu EC, Grama A and Necula C, 2001. Paleoclimatic record from loess-paleosol profile in Southeastern Romania. *Physics and Chemistry of the Earth* A (11-12): 893-898.

Panaiotu CE, Balescu S, Lamothe M, Panaiotu CG, Necula C and Grama A, 2004. Astronomical and luminescence dating of Lower Danubian loess (Romania). *Geophysical Research Abstracts* 6: 02900.

Poolton, N.R.J., Wallinga, J., Murray A.S., Bulur, E., Bøtter-Jensen L., 2002a. Electrons in feldspar I: on the wavefunction of electrons trapped at simple lattice defects. Physics and Chemistry Mineral 29, 210-216.

Poolton, N.R.J., Ozanyan K.B., Wallinga, J., Murray A.S., Bøtter-Jensen L., 2002b. Electrons in feldspar II: a consideration of the influence of conduction band-tail states on luminescence processes. Physics and Chemistry Mineral 29, 217-225.

Preusser, F., 2009. Quartz as a natural luminescence dosimeter. Eart-Science Reviews 97, 184-214.

Pye, K., 1995. The nature, origin and accumulation of loess. Quaternary Science Reviews 14, 653-667.

Roberts, H.M., 2008. The development and application of luminescence dating to loess deposits: a perspective on the past, present and future. Boreas 37, 483-507.

Roberts, H.M., Wintle, A.G., 2001. Equivalent dose determinations for polymineralic fine-grains using SAR protocol: application to a Holocene sequence of the Chinese Loess Plateau. Quaternary Science Reviews 20, 859-863.

Schmidt, E.D., Machalett, B., Marković, S.B., Tsukamoto, S., Frechen, M., 2010. Luminescence chronology of the upper part of the Stari Slankamen loess sequence (Vojvodina, Serbia). Quaternary Geochronology 5, 137-142.

Schmidt, E.D., Frechen, M., Murray, A.S., Tsukamoto, S., Bittmann F., 2011. Luminescence chronology of the loess record from the Tönchesberg section: A comparison using quartz and feldspar as dosimeter to extend the age range beyond the Eemian. Quaternary International 234, 10-22.

Smalley, I.J., Jefferson, I.F., Dijkstra, T.A., Derbyshire, E., 2001. Some major events in the development of the scientific study of loess. Earth Science Reviews 54, 5-18.

Spooner N.A., 1994. The anomalous fading of infrared-stimulated luminescence from feldspars. Radiation Measurements 23, 625-632.

Stevens, T., Thomas, D.S.G., Armitage, S.J., Lunn, H.R., Lu, H., 2007. Reinterpreting climate proxy records from Late Quaternary Chinese loess: A detailed OSL investigation. Earth-Science Reviews 80: 111-136.

Stevens, T., Marković, S.B., Zech, M., Hambach, U., Sümegi, P., 2011. Dust deposition and climate in the Carpathian Basin over an independently dated last glacial-interglacial cycle. Quaternary Science Reviews 30, 662-681.

Strickertsson, K., 1985. The thermoluminescence of potassium feldspars-glow curve characteristics and initial rise measurements. Nucl. Tracks 10, 613-617.

Thiel, C., Coltori, M., Tsukamoto, S., Frechen, M., 2010. Geochronology for some key sites along the coasts of Sardinia. Quaternary International 222, 36-47.

Thiel, C., Terhorst, B., Jaburová, I., Buylaert, J.P., Murray, A.S., Fladerer, F.A., Damm, b., Frechen, M., Ottner, F., 2011a. Sedimentation and erosion processes in Middle to Late Pleistocene sequences in the brickyard Langenlois/Lower Austria. Geomorphology doi:10.1016/j.geomorph.2011.02.011.

Thiel, C., Buylaert, J.P., Murray, A., Terhorst, B., Hofer, I.., Tsukamoto, S., Frechen, M., 2011b. Luminescence dating of the Stratzing loess profile (Austria) - Testing the potential of an elevated temperature post-IR IRSL protocol. Quaternary International 234, 23-31.

Thomsen, K.J., Murray, A.S., Jain, M., Bøtter-Jensen, L., 2008. Laboratory fading rates of various luminescence signals from feldspar-rich sediment extracts. Radiation Measurements 43, 1474-1486.

Thomsen, K.J., Murray, A.S., Jain, M., 2011. Stability of IRSL sigals from sedimentary K-feldspar samples. Geochronometria 38, 1-13.

Timar, A., Vandenberghe, D., Panaiotu, E.C., Panaiotu, C.G., Necula, C., Cosma, C., Van den haute, P., 2010. Optical dating of Romanian loess using fine-grained quartz. Quaternary Geochronology 5, 143-148.

Timar-Gabor, A.I., Vandenberghe, D.A.G., **Vasiliniuc, S.,** Panaiotu, C.E., Panaiotu, C.G., Dimofte, D., Cosma, C., 2011. Optical dating of Romanian loess: a comparison between sand-sized and silt-sized quartz. Quaternary International 240, 62-70.

Vandenberghe D, De Corte F, Buylaert J-P, Kučera J and Van den haute P, 2008. On the internal radioactivity in quartz. *Radiation Measurements* 41: 768-773.

Vasiliniuc, S., Timar-Gabor, A., Vandenberghe, D.A.G., Panaiotu, C.G., Begy, R.Cs., Cosma, C., 2011. A high resolution optical dating study of the Mostiştea loess-palaeosol sequence (SE Romania) using sand-sized quartz. Geochronometria 38, 34-41.

Vasiliniuc, S., Vandenberghe, D., Timar-Gabor, A., van den Haute, P., Cosma, C., submitted-a. Conventional IRSL dating of Romanian loess using single aliquots of polymineral fine grains. Radiation Measurements.

Vasiliniuc, S., Vandenberghe, D., Timar-Gabor, A., Cosma, C., van den Haute, P., submitted-b. Combined IRSL and post-IR OSL dating of Romanian loess using single aliquots of polymineral fine grains. Quaternary International.

Visocekas, R., 2002. Tunnelling in afterglow, its coexistence and interweaving with thermally stimulated luminescence. Radiation Protection Dosimetry 100, 45-54.

Wallinga, J., Murray, A., Duller, G., 2000. Underestimation of equivalent dose in single-aliquot optical dating of feldspars caused by preheating. Radiation Measurements 32, 691-695.

Wintle, A.G., 1973. Anomalous fading of thermoluminescence in mineral samples. Nature 245, 143-144.

Wintle, A.G., 2008. Luminescence dating: where it has been and where it is going. Boreas 37, 471-482.

Wintle, A.G., Murray, A.S., 2006. A review of quartz optically stimulated luminescence characteristics and their relevance in single-aliquot regeneration dating protocols. Radiation Measurements 41, 369-391.

Yoshida, H., Roberts, R.G., Olley, J.M., Laslett, G.M., Galbraith, R.F., 2000. Extending the age range of optical dating using single 'supergrains' of quartz. Radiation Measurements 32, 439-446.

Zöller, L., 2010. New approaches to European loess: a stratigraphic and methodical review of the past decade. Central European Journal of Geosciences 2, 19-31.